

Nambu-Covariant Many-Body Theory II: Self-Consistent Approximations

M. Drissi ^{1,*} A. Rios ^{1,2} and C. Barbieri ^{3,4,1}

¹*Department of Physics, University of Surrey, Guildford GU2 7XH, United Kingdom*

²*Departament de Física Quàntica i Astrofísica, Institut de Ciències del Cosmos (ICCUB),
Universitat de Barcelona, Martí Franquès 1, E08028 Barcelona, Spain*

³*Dipartimento di Fisica, Università degli Studi di Milano, Via Celoria, 16, I-20133 Milano, Italy*

⁴*INFN, Sezione di Milano, Via Celoria 16, I-20133 Milano, Italy*

(Dated: September 7, 2021)

This paper is devoted to the formulation of Self-Consistent Green's Function (SCGF) in an explicit Nambu-covariant fashion for applications to many-body systems at non-zero temperature in symmetry-broken phases. This is achieved by extending the Nambu-covariant formulation of perturbation theory, presented in the first part of this work, to non-perturbative schemes based on self-consistently dressed propagators and vertices. We work out in detail the self-consistent ladder approximation, motivated by a trade-off between numerical complexity and many-body phenomenology. Taking a complex general Hartree-Fock-Bogoliubov (HFB) propagator as the starting point, we also formulate and prove a sufficient condition on the stability of the HFB self-energy to ensure the convergence of the initial series of ladders at any energy. The self-consistent ladder approximation is written purely in terms of spectral functions and the resulting set of equations, when expressed in terms of Nambu tensors, are remarkably similar to those in the symmetry-conserving case. This puts the application of the self-consistent ladder approximation to symmetry-broken phases of infinite nuclear matter within reach.

I. INTRODUCTION

In the first part of this work, henceforth referred to as Part I [1], we have formulated the perturbative expansion of the Green's functions of a given many-body system in terms of Nambu tensors. This formulation, referred to as Nambu-Covariant Perturbation Theory (NCPT), allows for a straightforward design of Bogoliubov-invariant perturbative approximations of many-body observables. In Part I, we have also shown that the un-oriented Feynman diagrams, which index perturbative contributions in NCPT, factorise a multitude of Feynman diagrams that occur in other diagrammatic formalisms accounting for particle-number symmetry-breaking [2, 3]. In addition, we have argued that such factorisation can be used to develop new algorithms with improved scalability for massively parallel computational architectures. Nevertheless, as powerful as they are, approximations that remain perturbative in the bare interaction are not well suited to tackle strongly correlated many-body systems, including atomic nuclei and neutron-star matter. To overcome this difficulty, a multitude of approaches have been developed in *ab initio* nuclear physics.

A first strategy consists in improving the starting point of the perturbative expansion. This leads to the development of algorithms that tackle directly more and more complex model Hamiltonians. From a given Hamiltonian H , the aim is to design another Hamiltonian, H_{ref} , together with the means of calculating associated observables. H_{ref} is engineered such that the observables associated to it are as close as possible to those associated to H . This is the case, for example, of the No-Core Shell

Model [4–6] which aims at calculating eigenenergies and eigenstates of atomic nuclei via a partial diagonalisation of a given H_{ref} , which equals H on a carefully chosen model space. Another approach along these lines is mean-field theory, and its many refinements including spontaneous symmetry-breaking, projections and the Generator Coordinate Method [7]. These approaches ultimately amount to design an H_{ref} not equal to H , but optimised to best reproduce the ground-state energy of H associated to a system of interest. For a recent review combining projections and spontaneous symmetry-breaking in the theory of mean fields see Ref. [8]. Similarity Renormalisation Group techniques [9–11], and their in-medium counterparts like the In-Medium Similarity Renormalisation Group (IM-SRG) [12–15], can also be included in this line of research. A complementary strategy consists in building a series of corrections, depending on the difference $H - H_{\text{ref}}$, with the best possible rate of convergence to the exact value of the observables of interest. Standard Many-Body Perturbation Theory (MBPT), in its many flavours [16], is a prime example of this strategy. One can also treat complex many-body systems using summations of infinite subsets of Feynman diagrams. Among these refinements, we mention the Coupled Cluster (CC) [17–20] and Self-Consistent Green's Function (SCGF) approaches [21–24]. Additionally, the techniques of resummation of a series can also be included in this line of research as they aim at improving the rate of convergence of a given series. For example, let us mention the resummations based on analytic continuation or Padé approximants which are compared in Ref. [25].

Modern *ab initio* approaches have grown more sophisticated by hybridising several of the techniques mentioned above. To name a few of those recent hybridisations, we mention the combination of particle-number

* m.drissi@surrey.ac.uk

symmetry-breaking with MBPT, CC, SCGF and IMSRG which lead, respectively, to the development of Bogoliubov MBPT [26]; Bogoliubov CC [3, 27]; Gorkov SCGF [2, 28, 29] and Bogoliubov IMSRG [30]. In general, the aim of such hybridisation techniques is to increase the range of applicability while reducing the global numerical cost. The typical price to pay is the development of an increasingly complex formalism and a more intricate numerical implementation. For example, a reliable and precise calculation of thermodynamical properties of infinite superfluid nuclear matter is expected to require such a hybrid method. Neutron-star physics requires the application of an approach that can tackle anisotropic pairing gaps, which can be dealt with rotational and particle-number symmetry-breaking [31, 32]. Moreover, the strong repulsion (or hard core) of several nuclear interactions can be dealt with by performing an infinite, ladder diagrammatic summation [33–37]. Finally, to ensure the thermodynamical consistency of macroscopic observables computed *ab initio*, a SCGF approximation is required [38]. While this is not the only possible *ab initio* route to deal with the thermodynamics of superfluid nuclear matter, the combination of spontaneous symmetry-breaking, ladder diagrammatic summation, and self-consistent propagators at non-zero temperature represents a substantial step forward compared to existing treatments. Unsurprisingly, these requirements increase non-negligibly the formal complexity. To mitigate this complexity, one could use software to automatically expand more and more complex many-body approximations. For example, a software toolchain is under development which so far automatizes diagrammatic generation at zero temperature [39] and angular momentum reduction [40]. In our case, where we want to sum an infinite number of diagrams at non-zero temperature, automatized approaches in existence fall short and further developments are required.

Instead, we address directly the additional complexity at the formal level. In Part I, we reformulated the many-body problem in terms of Nambu tensors, which allowed us to derive approximations of many-body observables without specifying the extended basis we are working with. This extra mathematical abstraction not only allows us to derive equations valid up to any Bogoliubov transformation, but also removes an unnecessary surplus of formal complexity. The extended basis should be specified only when it brings necessary extra properties¹. In the case of the self-consistent ladder approximation at non-zero temperature with symmetry-breaking, this will lead to a self-consistent set of equations of similar complexity compared to the symmetry-conserving case.

The aim of this paper is therefore to formulate the theory of SCGF in a Nambu-covariant fashion. We refer to this particular approach of SCGF as Nambu-

Covariant Self-Consistent Green's Function (NC-SCGF). The present paper is organised as follows. In Sec. II, we derive exact properties of the propagator and emphasise their associated covariance group. Self-consistent approximations of the propagator are then expressed within the Nambu-covariant formalism in Sec. III. Finally, in Sec. IV, we study a self-consistent dressing of the two-body interaction via a Bethe-Salpeter equation [41]. We also derive the ladder approximation as a particular case. We defer the discussion of specific applications to infinite nuclear matter into a subsequent paper.

II. NAMBU TENSOR PROPAGATOR

In this section, we define the propagator for a given Hamiltonian, Ω , as a Nambu tensor. For simplicity, we assume that Ω is Hermitian and time-independent. We introduce the spectral representation of the propagator and detail the generalisation of standard exact properties to the symmetry-breaking case.

A. Definitions

1. Bases

Let us consider a many-body system of fermions in a statistical ensemble described by the Hermitian Hamiltonian Ω and the inverse temperature β . Let \mathcal{B}^e be a basis of the extended one-body Hilbert space $\mathcal{H}_1^e \equiv \mathcal{H}_1 \times \mathcal{H}_1^\dagger$, as discussed in Part I. For convenience, we choose to work with an extended basis \mathcal{B}^e comprised of an orthonormal single-particle basis, $\mathcal{B} = \{|b\rangle\}$, and its Hermitian conjugate, $\mathcal{B}^\dagger = \{\langle b|\}$, i.e.

$$\mathcal{B}^e \equiv \mathcal{B} \cup \mathcal{B}^\dagger. \quad (1)$$

We also index the extended basis over global indices

$$\mu \equiv (b, l_b) \quad (2)$$

where b indexes single-particle states, and l_b are Nambu indices. Despite working with a specific extended basis \mathcal{B}^e , most of the equations that follow will be equalities between two Nambu tensors. As such, the equations remain valid if one works in a different extended basis, $\mathcal{B}^{e'}$. In some particular cases, however, equations will be valid only for a subset of extended bases. In such cases, we will specify under the action of which sub-group of $\text{GL}(\mathcal{H}_1^e)$ the equations remain valid.

Let A^μ and \bar{A}_μ be Nambu fields associated to the

¹ For example, we will see that the Galitskii-Migdal-Koltun (GMK) sum rule as given in Eq. (46) is only valid for a certain subset of extended bases.

extended basis \mathcal{B}^e . These fields verify²

$$A^{(b,1)} \equiv a_b , \quad (3a)$$

$$A^{(b,2)} \equiv \bar{a}_b = a_b^\dagger , \quad (3b)$$

$$\bar{A}_{(b,1)} \equiv \bar{a}_b = a_b^\dagger , \quad (3c)$$

$$\bar{A}_{(b,2)} \equiv a_b , \quad (3d)$$

where \dagger denotes the usual Hermitian conjugation, and where $\bar{a}_b(a_b)$ denote creation (annihilation) operators associated to the orthonormal single-particle basis, \mathcal{B} . Let also $g^{\mu\nu}$ be the metric tensor verifying

$$\{ A^\mu, A^\nu \} = g^{\mu\nu} , \quad (4a)$$

$$\{ A^\mu, \bar{A}_\nu \} = g^\mu{}_\nu , \quad (4b)$$

$$\{ \bar{A}_\mu, \bar{A}_\nu \} = g_{\mu\nu} . \quad (4c)$$

We recall that the metric tensor can be used to raise or lower indices,

$$A^\mu = \sum_\nu g^{\mu\nu} \bar{A}_\nu , \quad (5a)$$

$$\bar{A}_\mu = \sum_\nu g_{\mu\nu} A^\nu , \quad (5b)$$

and that it fulfils the relation

$$\sum_\lambda g^{\mu\lambda} g_{\lambda\nu} = g^\mu{}_\nu = \delta_{\mu\nu} . \quad (6)$$

For more details on the foundations of the Nambu-covariant formalism, we refer the reader to Part I.

2. Nambu tensor propagator

The Hamiltonian Ω is expressed as a polynomial of contravariant Nambu fields according to

$$\Omega \equiv \sum_{k=0}^{k_{\max}} \frac{1}{(2k)!} \sum_{\mu_1 \dots \mu_{2k}} v_{\mu_1 \dots \mu_{2k}}^{(k)} A^{\mu_1} \dots A^{\mu_{2k}} , \quad (7)$$

where $v_{\mu_1 \dots \mu_{2k}}^{(k)}$ are covariant Nambu tensors. We note that k denotes the k -body nature of the tensor, in the sense that it involves $2k$ Nambu fields. In the symmetry-conserving case, $k = 2$ would be associated to a two-body interaction; $k = 3$, to a three-body interaction, and so on.

The exact contravariant, mixed and covariant versions of the Nambu tensor propagator are defined by³

$$-\mathcal{G}^{\mu\nu}(\tau, \tau') \equiv \langle T [A^\mu(\tau) A^\nu(\tau')] \rangle , \quad (8a)$$

$$-\mathcal{G}^\mu{}_\nu(\tau, \tau') \equiv \langle T [A^\mu(\tau) \bar{A}_\nu(\tau')] \rangle , \quad (8b)$$

$$-\mathcal{G}_\mu{}^\nu(\tau, \tau') \equiv \langle T [\bar{A}_\mu(\tau) A^\nu(\tau')] \rangle , \quad (8c)$$

$$-\mathcal{G}_{\mu\nu}(\tau, \tau') \equiv \langle T [\bar{A}_\mu(\tau) \bar{A}_\nu(\tau')] \rangle , \quad (8d)$$

where the imaginary-time dependence is with respect to Ω and where $T[\dots]$ denotes the time-ordering from right to left when increasing imaginary-time τ . The ensemble average $\langle \dots \rangle$ is defined with respect to Ω . The exact density matrix, ρ , and the partition function, Z , are defined by

$$\rho \equiv \frac{1}{Z} e^{-\beta\Omega} , \quad (9a)$$

$$Z \equiv \text{Tr} (e^{-\beta\Omega}) . \quad (9b)$$

We stress that the raising and lowering of indices via metric contractions is compatible with the definitions given in Eqs. (8). For instance, the fully covariant and fully contravariant propagators are related by the expression

$$\mathcal{G}^{\mu\nu}(\tau, \tau') = \sum_{\lambda_1 \lambda_2} g^{\mu\lambda_1} g^{\nu\lambda_2} \mathcal{G}_{\lambda_1 \lambda_2}(\tau, \tau') . \quad (10)$$

In the following, most equations will remain valid after any raising/lowering of indices. Whenever there is no ambiguity, we choose to drop tensor indices and write equalities between tensors in an intrinsic fashion.

Since we assume Ω to be time-independent, the propagator depends only on the difference of its two times and we can use, without ambiguity, the one-time notation

$$\mathcal{G}(\tau) \equiv \mathcal{G}(\tau + \tau', \tau') = \mathcal{G}(\tau, 0) . \quad (11)$$

The exact propagator verifies an antisymmetry property, and is extended into a β -quasiperiodic function so that

$$\mathcal{G}^{\mu\nu}(\tau) = -\mathcal{G}^{\nu\mu}(-\tau) , \quad (12a)$$

$$\mathcal{G}^{\mu\nu}(\tau + \beta) = -\mathcal{G}^{\nu\mu}(\tau) . \quad (12b)$$

These equations remain valid under the action of $\text{GL}(\mathcal{H}_1^e)$. The propagator also fulfils the Hermitian property,

$$\mathcal{G}^{\mu\nu}(\tau)^* = \mathcal{G}_{\nu\mu}(\tau) , \quad (12c)$$

which, however, remains valid only under the action of the unitary group $\text{U}(\mathcal{H}_1^e)$. As discussed in App. A, we replace Eq. (12c) with

$$(\mathcal{G}^\dagger)^{\mu\nu}(\tau) = \mathcal{G}^{\mu\nu}(\tau) \quad (12d)$$

² We stress that, in a general extended basis $\mathcal{B}^{e'}$, Nambu fields are linear combinations of creation and annihilation operators. In addition, without the assumed orthonormality of \mathcal{B} , creation and annihilation operators would not be Hermitian conjugated to each other. See Part I for more details.

³ As for Part I, we assume natural units where $\hbar = c = k_B = 1$.

where \dagger denotes the Hermitian conjugation of a tensor as defined in App. A. The advantage of Eq. (12d) over Eq. (12c) is that it remains valid under the action of $GL(\mathcal{H}_1^e)$. With this, we can write the antisymmetry, β -quasiperiodic and Hermitian properties of the propagator in an intrinsic fashion as

$$\mathcal{G}^\top(\tau) = -\mathcal{G}(-\tau), \quad (13a)$$

$$\mathcal{G}(\tau + \beta) = -\mathcal{G}^\top(\tau), \quad (13b)$$

$$\mathcal{G}^\dagger(\tau) = \mathcal{G}(\tau), \quad (13c)$$

where \top denotes the transposition defined in Part I.

As a consequence of Eqs. (13), we can define the energy representation of the exact propagator as the following Fourier transform

$$\mathcal{G}(\omega_p) \equiv \int_0^\beta d\tau e^{i\omega_p \tau} \mathcal{G}(\tau), \quad (14a)$$

$$\mathcal{G}(\tau) = \frac{1}{\beta} \sum_p e^{-i\omega_p \tau} \mathcal{G}(\omega_p), \quad (14b)$$

where $\omega_p \equiv (2p + 1)\frac{\pi}{\beta}$ are fermionic Matsubara frequencies. In the energy representation, the Hermitian and antisymmetry properties read

$$\mathcal{G}(\omega_p) = \mathcal{G}^\dagger(-\omega_p), \quad (15a)$$

$$\mathcal{G}(\omega_p) = -\mathcal{G}^\top(-\omega_p). \quad (15b)$$

B. Spectral representation

Let $|\Psi_n\rangle$ and Ω_n denote exact orthonormal eigenstates and real eigenvalues of Ω , i.e.

$$\forall n, \Omega |\Psi_n\rangle = \Omega_n |\Psi_n\rangle. \quad (16)$$

The set of $|\Psi_n\rangle$ forms a complete basis of the Fock space. Using this orthonormal basis to express traces over Fock space, the Fourier transform of the exact propagator reads

$$\begin{aligned} \mathcal{G}^{\mu\nu}(\omega_p) &= \frac{1}{Z} \sum_{m,n} \langle \Psi_m | A^\mu | \Psi_n \rangle \langle \Psi_n | A^\nu | \Psi_m \rangle \\ &\quad \times e^{-\beta\Omega_m} \frac{e^{-\beta(\Omega_n - \Omega_m)} + 1}{i\omega_p - (\Omega_n - \Omega_m)}, \end{aligned} \quad (17)$$

which is the so-called Lehman's representation of the propagator. Defining the spectral function by

$$\begin{aligned} S^{\mu\nu}(\omega) &\equiv \frac{1}{Z} \sum_{m,n} \langle \Psi_m | A^\mu | \Psi_n \rangle \langle \Psi_n | A^\nu | \Psi_m \rangle \\ &\quad \times e^{-\beta\Omega_m} (1 + e^{-\beta\omega}) 2\pi \delta(\Omega_n - \Omega_m - \omega), \end{aligned} \quad (18)$$

the *spectral representation* of the propagator reads

$$\mathcal{G}(\omega_p) = \int_{-\infty}^{+\infty} \frac{d\omega'}{2\pi} \frac{S(\omega')}{i\omega_p - \omega'}. \quad (19)$$

The spectral function verifies the Hermitian and antisymmetry properties

$$S(\omega) = S^\dagger(\omega), \quad (20a)$$

$$S(\omega) = S^\top(-\omega). \quad (20b)$$

From the spectral function, we define the analytic propagator $\mathcal{G}(z)$ as the Nambu tensor verifying

$$\mathcal{G}(z) \equiv \int_{-\infty}^{+\infty} \frac{d\omega'}{2\pi} \frac{S(\omega')}{z - \omega'}, \quad (21)$$

where the energy z is now generically complex. This analytic continuation into the complex plane is unique [42], so long as the tensor coordinates are functions of energy that are analytic off the real axis, vanish at infinity and verify

$$\mathcal{G}^{\mu\nu}(z = i\omega_p) = \mathcal{G}^{\mu\nu}(\omega_p). \quad (22)$$

The spectral function is recovered from the analytic propagator as the discontinuity across the real axis,

$$S(\omega) = i [\mathcal{G}(z = \omega + i\eta) - \mathcal{G}(z = \omega - i\eta)], \quad (23)$$

where ω is a real frequency and η is to be understood in the limit $\lim_{\eta \rightarrow 0^+}$. The Hermitian and antisymmetry properties of the analytic propagator read

$$\mathcal{G}(z) = \mathcal{G}^\dagger(z^*), \quad (24a)$$

$$\mathcal{G}(z) = -\mathcal{G}^\top(-z). \quad (24b)$$

From the analytic propagator, we define the retarded and advanced propagators as the Nambu tensors verifying

$$G^{R/A}(\omega) = \mathcal{G}(z = \omega \pm i\eta). \quad (25)$$

In other words, retarded (advanced) components of the propagator are obtained as the limits toward the real axis of the analytic propagator in the complex upper (lower) halfplane. The retarded and advanced propagators verify the Hermitian and antisymmetry properties

$$G^R(\omega) = G^{A\dagger}(\omega), \quad (26a)$$

$$G^R(\omega) = -G^{A\top}(-\omega). \quad (26b)$$

The retarded and advanced propagators can be recovered directly from the spectral function by plugging Eq. (21) into Eq. (25), so that

$$G^{R/A}(\omega) = \int_{-\infty}^{+\infty} \frac{d\omega'}{2\pi} \frac{S(\omega')}{\omega - \omega' \pm i\eta}. \quad (27)$$

Combining Eq. (27) and the Sokhotski-Plemelj identity

$$\frac{1}{x \pm i\eta} = \mathcal{P} \frac{1}{x} \mp i\pi\delta(x), \quad (28)$$

we obtain the following dispersion relations

$$\overline{\text{Re}} G^{R/A}(\omega) = \mathcal{P} \int_{-\infty}^{+\infty} \frac{d\omega'}{2\pi} \frac{S(\omega')}{\omega - \omega'}, \quad (29a)$$

$$\overline{\text{Im}} G^{R/A}(\omega) = \mp \frac{1}{2} S(\omega), \quad (29b)$$

where \mathcal{P} denotes the principal value and where

$$\overline{\text{Re}} t \equiv \frac{t + t^\dagger}{2}, \quad (30a)$$

$$\overline{\text{Im}} t \equiv \frac{t - t^\dagger}{2i}, \quad (30b)$$

define respectively the Hermitian and anti-Hermitian parts of a tensor t , which are proper Nambu tensors. Conversely, we can find t and its Hermitian conjugate, t^\dagger , from its Hermitian and anti-Hermitian parts

$$t = \overline{\text{Re}} t + i \overline{\text{Im}} t, \quad (31a)$$

$$t^\dagger = \overline{\text{Re}} t - i \overline{\text{Im}} t. \quad (31b)$$

We note that, compared to the standard symmetry-conserving case [43, 44], the real and imaginary parts appearing in the dispersion relations have been replaced by Hermitian and anti-Hermitian parts.

C. Sum rules and positivity bounds

In addition to the symmetries described by Eqs. (20), the spectral function of the propagator verifies additional exact properties which take the form of sum rules and positivity bounds. The energy weighted sum rules relate the different moments of the spectral function, $S(\omega)$, to the Hamiltonian, Ω . The 0th moment is deduced from the anticommutation rule in Eq. (4a) and reads

$$\int_{-\infty}^{+\infty} \frac{d\omega}{2\pi} S(\omega) = g. \quad (32)$$

More generally, the n^{th} moment of the spectral function satisfies the relation

$$m_n = \int_{-\infty}^{+\infty} \frac{d\omega}{2\pi} \omega^n S^{\mu\nu}(\omega) = \left\langle \left\{ \underbrace{[\dots [A^\mu, \Omega], \dots, \Omega], A^\nu}_{n \text{ commutators}} \right\} \right\rangle, \quad (33)$$

where the right-hand side defines the thermal average of a series of n nested commutators involving A^μ and Ω , and an additional anti-commutator with A^ν .

An interesting property of the spectral representation is the relation between the moments of the spectral function and the asymptotic expansion around infinity of the analytic propagator. For any $n \in \mathbb{N}$, we find

$$\mathcal{G}(z) = \sum_{k=0}^n \frac{m_k}{z^{k+1}} + O\left(\frac{1}{z^{n+2}}\right). \quad (34)$$

For $n = 0$, we recover the well known asymptotic behaviour of the diagonal components

$$\mathcal{G}^\mu_\mu(z) = \frac{1}{z} + O\left(\frac{1}{z^2}\right), \quad (35)$$

while the asymptotic behaviour of the off-diagonal components verify

$$\mathcal{G}^\mu_\nu(z) = \frac{(m_1)^\mu_\nu}{z^2} + O\left(\frac{1}{z^3}\right), \quad (36)$$

with $\mu \neq \nu$ ⁴. We stress that the diagonal and off-diagonal components of the (1,1)-type propagator have different asymptotic behaviours when $|z| \rightarrow \infty$.

Another important sum rule is the so-called Galitskii-Migdal-Koltun (GMK) sum rule [45, 46], which connects the one-body spectral function to the expectation value of the Hamiltonian. We emphasise that the validity of this sum rule, as given here, depends on the choice of the extended basis. In other words, the sum rule is not an equality between two Nambu tensors.

The GMK sum rule stems from the following relation between a sum of commutators of Nambu tensors and the Hamiltonian,

$$-\sum_{\mu} \langle [\bar{A}_\mu, \Omega] A^\mu \rangle = \sum_{k=1}^{k_{\max}} \frac{1}{(2k-1)!} \sum_{\mu_1 \dots \mu_{2k}} v_{[\mu_1 \dots \mu_{2k-1} \mu_{2k}]^{(k)}} \langle A^{\mu_1} \dots A^{\mu_{2k}} \rangle. \quad (37)$$

On the right-hand side, the partially antisymmetric part of a k -body interaction, $v_{[\mu_1 \dots \mu_{2k-1} \mu_{2k}]^{(k)}}$, appears. This partially antisymmetric part is defined by

$$v_{[\dots \dot{\mu}_1 \dots \dot{\mu}_2 \dots \dot{\mu}_p \dots]^{(k)}} \equiv \frac{p!}{(2k)!} \sum_{\sigma \in S_{2k}/S_p} \epsilon(\sigma) v_{\mu_{\sigma(1)} \dots \mu_{\sigma(2k)}}^{(k)}, \quad (38)$$

where S_{2k}/S_p is the set of permutations of the $2k$ indices keeping the order of the p dotted indices fixed. More details about totally and partially antisymmetrisations are given in Part I of our work. The problem in establishing a GMK-type sum rule is that, in general, the partially antisymmetric parts are different from the original interaction terms,

$$v_{[\mu_1 \dots \dot{\mu}_{2k-1} \mu_{2k}]^{(k)}} \neq v_{\mu_1 \dots \mu_{2k-1} \mu_{2k}}^{(k)}, \quad (39)$$

which would normally appear in the expectation value of the energy.

⁴ Eq. (36) is an equality between tensor coordinates, but not all of them. The equality does not hold when $\mu = \nu$. Thus Eq. (36) should not be understood as an equality of tensors. Any associated raising or lowering of indices requires extra care.

To go further, we rely on the fact that, in our particular choice of extended basis, defined in Eq. (1), Nambu fields are either pure creation or pure annihilation operators of single-particle states. We therefore use Eqs. (3), combined with the assumption that Ω conserves the number of particles, to show that

$$-\sum_c \left\langle [\bar{A}_{(c,1)}, \Omega] A^{(c,1)} \right\rangle = \sum_{k=1}^{k_{\max}} k \left\langle \Omega^{[k]} \right\rangle, \quad (40)$$

where $\Omega^{[k]}$ represents an individual k -body term in the Hamiltonian, Eq. (7), i.e.

$$\Omega^{[k]} \equiv \frac{1}{(2k)!} \sum_{\mu_1 \dots \mu_{2k}} v_{\mu_1 \dots \mu_{2k}}^{(k)} A^{\mu_1} \dots A^{\mu_{2k}}. \quad (41)$$

Note that in Eq. (40) the contraction is only made on the single-particle index c so that the resulting term is *not* a Nambu scalar tensor. We emphasise this aspect using the explicit (b, l_b) notation, rather than the global indices, μ . Assuming a two-body interaction only, $k_{\max} = 2$, we have

$$\begin{aligned} \langle \Omega \rangle &= \langle \Omega^{[1]} \rangle + \langle \Omega^{[2]} \rangle \\ &= \frac{1}{2} \langle \Omega^{[1]} \rangle + \frac{1}{2} \sum_{k=1}^{k_{\max}} k \langle \Omega^{[k]} \rangle. \end{aligned} \quad (42)$$

The $k = 1$ term can be computed directly as an expectation value over the propagator. Using the spectral representation of the propagator, one can show that

$$\langle \Omega^{[1]} \rangle = \sum_{bc} \int_{-\infty}^{+\infty} \frac{d\omega}{2\pi} v^{(1)(b,1)}_{(c,1)} f(-\omega) S^{(c,1)}_{(b,1)}(-\omega) \quad (43)$$

where $f(\omega) \equiv \frac{1}{1+e^{\beta\omega}}$ is the Fermi-Dirac distribution. This distribution arises when performing the Matsubara sum in

$$\left\langle \bar{A}_{(b,1)} A^{(c,1)} \right\rangle = -\frac{1}{\beta} \sum_{\omega_p} \mathcal{G}_{(b,1)}^{(c,1)}(\omega_p) e^{-i\omega_p \eta}, \quad (44)$$

after the propagator has been replaced by its spectral representation. The negative sign in the argument of the spectral function is a consequence of our use of Eq. (20b) to make appear $S^{(c,1)}_{(b,1)}(-\omega)$ instead of $S_{(b,1)}^{(c,1)}(\omega)$. Since $v^{(1)}$ encodes the one-body part of the Hamiltonian, it typically includes kinetic terms and mean-field-like potentials.

Similarly, the expectation value in Eq. (40) reads

$$-\sum_c \left\langle [\bar{A}_{(c,1)}, \Omega] A^{(c,1)} \right\rangle = \sum_c \int_{-\infty}^{+\infty} \frac{d\omega}{2\pi} \omega f(-\omega) S^{(c,1)}_{(c,1)}(-\omega). \quad (45)$$

Combining Eqs. (42), (43) and (45), we find the GMK sum rule at non-zero temperature with symmetry-breaking,

namely

$$\begin{aligned} \langle \Omega \rangle &= \frac{1}{2} \sum_{bc} \int_{-\infty}^{+\infty} \frac{d\omega}{2\pi} f(-\omega) S^{(c,1)}_{(b,1)}(-\omega) \\ &\quad \times \left(v^{(1)(b,1)}_{(c,1)} + \omega \delta_{bc} \right). \end{aligned} \quad (46)$$

In the zero-temperature limit, we recover the same sum rule given by the Gorkov-Green's function formalism in Ref. [2]. This is also formally equivalent to the finite-temperature GMK sum rule obtained in the symmetry-conserving case [47–49]. We stress that the minus sign in the argument of $S(\omega)$ is a result of our choice of index ordering, and that $v^{(1)}$ includes also non-interacting components like the kinetic energy.

The GMK sum rule in Eq. (46) is only valid for a Hamiltonian conserving the particle-number symmetry and containing only two-body interactions. An extension to include three-body interactions may be derived following the steps drawn for non-superfluid systems in Ref. [50]. To derive this equation, we also have relied on the fact that we work in an extended basis, \mathcal{B}^e , which is the concatenation of two single-particle bases as given in Eq. (1). The latter implies that the GMK sum rule, as given in Eq. (46), remains invariant under the action of the sub-group $\text{GL}(\mathcal{H}_1)$ but not under the action of the whole group $\text{GL}(\mathcal{H}_1^e)$.

In addition to symmetry properties and sum rules, the exact spectral function of the propagator fulfils a series of relevant positivity inequalities. From the spectral function in Eq. (18), we can show that, for any $(1, 0)$ -tensor X and any orthogonal extended basis,

$$\sum_{\mu\nu} (X^\mu)^* S^\mu_\nu(\omega) X^\nu > 0. \quad (47)$$

Eq. (20a) together with the previous equality amount to state that *the spectral function is Hermitian definite positive*. As a shorthand notation to denote Hermitian definite positiveness, we write

$$S(\omega) \succ 0. \quad (48)$$

In practice, the positive definiteness of $S(\omega)$ is equivalent to stating that all the principal minors of the matrix obtained from the tensor coordinates $S^\mu_\nu(\omega)$ in any orthogonal extended basis $\mathcal{B}^{e'l}$ are strictly positive.

In our case, we work in an extended basis \mathcal{B}^e which is orthogonal, as discussed in App. A. For the first principal minors, Hermitian definite positiveness means that

$$\forall \mu, S^\mu_\mu(\omega) > 0. \quad (49)$$

The inequality (49) is equivalent to the standard positivity property obtained in the symmetry-conserving case which, together with the sum rule in Eq. (32), endows the (diagonal elements) of the spectral function with a probabilistic interpretation [44]. In the symmetry-conserving case, the spectral function is diagonal and only the first principal

minors are setting non-trivial constraints on the spectral function. In the symmetry-breaking case, in contrast, the positivity condition of higher principal minors yields a set of non-trivial inequalities that must be fulfilled. As an example, from the positivity of the second principal minors, we find that the spectral function must satisfy

$$\forall \mu \neq \nu, |S^\mu_\nu(\omega)| < \sqrt{S^\mu_\mu(\omega)S^\nu_\nu(\omega)}, \quad (50)$$

where the Hermitian property of the spectral function, Eq. (20a), has been used together with the orthogonality of \mathcal{B}^e .

We stress that inequalities (49) and (50) remain valid only up to the action of the sub-group $U(\mathcal{H}_1^e)$. For more details on the orthogonality of an extended basis and the unitary group $U(\mathcal{H}_1^e)$ see App. A. In our case, where \mathcal{B}^e is the concatenation of two orthonormal single-particle bases, inequality (50) can be recast as

$$\left| S^{(b,1)}_{(c,2)}(\omega) \right| < \sqrt{S^{(b,1)}_{(b,1)}(\omega)S^{(c,2)}_{(c,2)}(\omega)}, \quad (51a)$$

$$\left| S^{(b,1)}_{(b,2)}(\omega) \right| < \sqrt{S^{(b,1)}_{(b,1)}(\omega)S^{(b,2)}_{(b,2)}(\omega)}, \quad (51b)$$

$$\left| S^{(b,1)}_{(c,1)}(\omega) \right| < \sqrt{S^{(b,1)}_{(b,1)}(\omega)S^{(c,1)}_{(c,1)}(\omega)}. \quad (51c)$$

We note that the positivity of higher minors yields additional bounds, that are not displayed here for conciseness.

III. SELF-CONSISTENT PROPAGATOR

In the previous section, we have introduced a series of properties for the exact propagator in a manifestly Nambu-covariant fashion. In this section, we study self-consistent approximations to the propagator, much as one would do in the symmetry-conserving case. First, we introduce the self-energy via a Dyson-Schwinger equation. We also detail its analytical properties, which are useful in applications. Second, we introduce specific approximations of the self-energy which lead to self-consistent approximations for the propagator. Last, we use the Hartree-Fock-Bogoliubov (HFB) approximation as an example of such self-consistent approximations.

A. Dyson-Schwinger equation

Let us first consider the partitioning of the Hamiltonian

$$\Omega \equiv \Omega_0 + \Omega_1, \quad (52a)$$

$$\Omega_0 \equiv \frac{1}{2} \sum_{\mu\nu} U_{\mu\nu} A^\mu A^\nu, \quad (52b)$$

$$\Omega_1 \equiv \sum_{k=0}^{k_{\max}} \frac{1}{(2k)!} \sum_{\mu_1 \dots \mu_{2k}} v_{\mu_1 \dots \mu_{2k}}^{(k)} A^{\mu_1} \dots A^{\mu_{2k}}, \quad (52c)$$

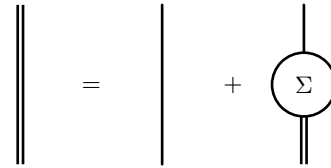


FIG. 1. Diagrammatic representation of the first Dyson-Schwinger equation given in Eqs. (54). The unperturbed propagator $\mathcal{G}^{(0)}$ and the exact propagator \mathcal{G} are represented by simple and double plain lines, respectively.

with the assumption that $U_{\mu\nu}$ is traceless and antisymmetric⁵.

The Dyson-Schwinger equation relates the exact propagator to the unperturbed one. The unperturbed analytic propagator $\mathcal{G}^{(0)}(z)$ is defined as the analytic propagator associated to Ω_0 . The analytic self-energy $\Sigma(z)$ associated to the partitioning of Eq. (52) is defined as the Nambu tensor verifying⁶

$$\Sigma(z) \equiv \mathcal{G}^{(0)-1}(z) - \mathcal{G}^{-1}(z). \quad (53)$$

Consequently, the analytic self-energy is related to the exact and unperturbed propagators via the *Dyson-Schwinger* equations

$$\mathcal{G}(z) = \mathcal{G}^{(0)}(z) + \mathcal{G}^{(0)}(z) \Sigma(z) \mathcal{G}(z) \quad (54a)$$

$$\mathcal{G}(z) = \mathcal{G}^{(0)}(z) + \mathcal{G}(z) \Sigma(z) \mathcal{G}^{(0)}(z). \quad (54b)$$

In the previous equation, the inverse of a tensor $\mathcal{G}^{-1}(z)$ and the products of tensors $\mathcal{G}^{(0)}(z)\Sigma(z)\mathcal{G}(z)$ are to be understood as functions of tensors as defined in App. B. As such, the products of tensors involve implicit sums over global indices that we do not make explicit for the sake of conciseness.

We show the first equation in Eqs. (54) in Fig. 1 using un-oriented Feynman diagrams. From now on, whenever there is no ambiguity, un-oriented Feynman diagrams obtained from the diagrammatics detailed in Part I will be simply referred to as Feynman diagrams.

If the Hamiltonian is a quadratic polynomial of Nambu fields, the propagator can be explicitly computed. For example, the unperturbed propagator, associated to Ω_0 defined in Eq. (52b) reads

$$\mathcal{G}^{(0)}(z) = (z - U)^{-1}. \quad (55)$$

In the case of the exact propagator associated to Ω , the explicit expression of the propagator depends on the self-energy,

$$\mathcal{G}(z) = (z - (U + \Sigma(z)))^{-1}. \quad (56)$$

⁵ This assumption can be made without loss of generality to the price of shifting Ω by a global constant. For more details, see Part I.

⁶ The analytic self-energy $\Sigma(z)$ denotes a tensor of type $p + q = 2$. To simplify notations, we use whenever possible the intrinsic notation, $\Sigma(z)$, as we did for the propagator and its spectral function.

In analogy to the propagator, the retarded, advanced, and imaginary-frequency components of the self-energy are obtained from the analytic self-energy $\Sigma(z)$ by

$$\Sigma^{R/A}(\omega) \equiv \Sigma(z = \omega \pm i\eta) , \quad (57a)$$

$$\Sigma(\omega_p) \equiv \Sigma(z = i\omega_p) , \quad (57b)$$

where ω_p are fermionic Matsubara frequencies.

Finally, although we mostly focus on the energy representation of the self-energy, it will be sometimes convenient to use the imaginary-time representation, $\Sigma(\tau, \tau')$. Like the propagator, the self-energy only depends on the time difference, $\tau - \tau'$. The energy representation is thus related to the time components via the Fourier transform

$$\Sigma(\omega_p) \beta \delta_{\omega_p, -\omega'_p} \equiv \int_0^\beta d\tau \int_0^\beta d\tau' e^{i\omega_p \tau} e^{i\omega'_p \tau'} \Sigma(\tau, \tau') , \quad (58a)$$

$$\Sigma(\omega_p) = \int_0^\beta d\tau e^{i\omega_p \tau} \Sigma(\tau) , \quad (58b)$$

where $\Sigma(\tau) \equiv \Sigma(\tau, 0)$. For completeness, we provide the Dyson-Schwinger equations in the time representation

$$\begin{aligned} \mathcal{G}(\tau, \tau') &= \mathcal{G}^{(0)}(\tau, \tau') \\ &+ \int_0^\beta d\tau_1 d\tau_2 \mathcal{G}^{(0)}(\tau, \tau_1) \Sigma(\tau_1, \tau_2) \mathcal{G}(\tau_2, \tau') , \end{aligned} \quad (59a)$$

$$\begin{aligned} \mathcal{G}(\tau, \tau') &= \mathcal{G}^{(0)}(\tau, \tau') \\ &+ \int_0^\beta d\tau_1 d\tau_2 \mathcal{G}(\tau, \tau_1) \Sigma(\tau_1, \tau_2) \mathcal{G}^{(0)}(\tau_2, \tau') . \end{aligned} \quad (59b)$$

B. Properties of the exact self-energy

The tensor coordinates of the self-energy are analytic in the upper and lower complex energy half-planes. Similarly as for the propagator, a spectral representation for the self-energy can be derived. First, we decompose the self-energy into an instantaneous (energy-independent) part and a continuous (energy-dependent, and vanishing at infinity) part,

$$\Sigma_{\mu\nu}(z) \equiv \Sigma_{\mu\nu}^\infty + \Sigma_{\mu\nu}^C(z) , \quad (60)$$

$$\lim_{|z| \rightarrow \infty} \Sigma_{\mu\nu}^C(z) \equiv 0 . \quad (61)$$

The instantaneous and continuous part of the self-energy are proper Nambu tensors. The continuous part has a

spectral representation, namely⁷

$$\Sigma^C(z) \equiv \int_{-\infty}^{+\infty} \frac{d\omega}{2\pi} \frac{\Gamma(\omega)}{z - \omega} , \quad (62)$$

where $\Gamma(\omega)$ is a Nambu tensor commonly referred to as the *width* of the self-energy. Plugging Eq. (62) into Eq. (60), the *spectral representation of the self-energy* reads

$$\Sigma(z) = \Sigma^\infty + \int_{-\infty}^{+\infty} \frac{d\omega}{2\pi} \frac{\Gamma(\omega)}{z - \omega} . \quad (63)$$

Similarly to the asymptotic expansion of the propagator, Eq. (34), an asymptotic expansion can be worked out for the self-energy,

$$\Sigma(z) = \Sigma^\infty + \sum_{k=0}^n \frac{s_k}{z^{k+1}} + O\left(\frac{1}{z^{n+2}}\right) , \quad (64)$$

as a function of the moments of the width, s_k , defined by

$$s_k \equiv \int_{-\infty}^{+\infty} \frac{d\omega}{2\pi} \omega^k \Gamma(\omega) , \quad (65)$$

for any $k \in \mathbb{N}$. The width can be recovered from the discontinuity of the analytic self-energy across the real axis,

$$\Gamma(\omega) = i [\Sigma(z = \omega + i\eta) - \Sigma(z = \omega - i\eta)] . \quad (66)$$

From the Hermitian and antisymmetry properties of the propagators, and from the Dyson-Schwinger equations (54) relating the self-energy to the propagators, we can obtain useful symmetry properties of the self-energy. For the analytic self-energy, these symmetry properties read

$$\Sigma(z) = \Sigma^\dagger(z^*) , \quad (67a)$$

$$\Sigma(z) = -\Sigma^\top(-z) . \quad (67b)$$

As a consequence, we have the following relations between the retarded and advanced components of the self-energy,

$$\Sigma^R(\omega) = \Sigma^{A\dagger}(\omega) , \quad (68a)$$

$$\Sigma^R(\omega) = -\Sigma^{A\top}(-\omega) . \quad (68b)$$

From these, one finds that

$$\overline{\text{Im}} \Sigma^\infty = \overline{\text{Im}} \Gamma(\omega) = 0 , \quad (69)$$

⁷ Here we are assuming for simplicity that $\forall \mu, \nu, \Sigma_{\mu\nu}^C(z) = o(\frac{1}{z})$. A counterexample of the spectral representation of Eq. (62) is given in chapter 14 of Ref. [51]. Note, however, that a generalised integral representation always holds. We refer the reader to Ref. [52] for more details on necessary and sufficient conditions to have a spectral representation.

or, in other words, the instantaneous self-energy and the width are necessarily Hermitian. Since the retarded and advanced self-energies are Hermitian conjugates of each other, it is convenient to define their common Hermitian part $R(\omega)$

$$R(\omega) \equiv \overline{\text{Re}} \Sigma^R(\omega) = \overline{\text{Re}} \Sigma^A(\omega) , \quad (70)$$

so that

$$\Sigma^{R/A}(\omega) = R(\omega) \mp i \frac{1}{2} \Gamma(\omega) . \quad (71)$$

Finally, we note that the width also fulfils a series of interesting symmetry and positivity properties⁸:

$$\Gamma(\omega) = \Gamma^\dagger(\omega) , \quad (73a)$$

$$\Gamma(\omega) = \Gamma^\top(-\omega) , \quad (73b)$$

$$\Gamma(\omega) \succ 0 . \quad (73c)$$

We stress, in particular, that Eqs. (73a) and (73c) means that the width is Hermitian positive definite.

From the previous properties, the relation between the width and the retarded and advanced self-energies takes the form of the often-used dispersion relations

$$\overline{\text{Re}} \Sigma^{R/A}(\omega) = \Sigma^\infty + \mathcal{P} \int_{-\infty}^{+\infty} \frac{d\omega'}{2\pi} \frac{\Gamma(\omega')}{\omega - \omega'} , \quad (74a)$$

$$\overline{\text{Im}} \Sigma^{R/A}(\omega) = \mp \frac{1}{2} \Gamma(\omega) . \quad (74b)$$

As usual, these dispersion relations can be used to build the full retarded or advanced components only from Σ^∞ and $\Gamma(\omega)$.

C. From the self-energy to the spectral function

In this subsection, we look at the relation between the the spectral function of the propagator, $S(\omega)$, and the width $\Gamma(\omega)$, combined with the instantaneous self-energy Σ^∞ . We derive two different sets of relations. First, we provide the general relations between the energy moments of these quantities. Then, we work out a direct relationship between these two tensors, leading us to refine the traditional physical interpretation of the spectral function.

⁸ The Hermitian definite positiveness property of the width is the least trivial one to derive. It stems from the Hermitian definite positiveness property of the spectral function $S(\omega)$ combined with Eq. (80) reformulated into

$$S(\omega) = G^R(\omega) \Gamma(\omega) G^{R\dagger}(\omega) . \quad (72)$$

1. Relations between energy moments

As discussed in Ref. [53] for the symmetry-conserving case, the energy moments of the spectral function, m_k , and of the width, s_k , are related to each other. A link can be established by matching the asymptotic expansion of the propagator, Eq. (34), to the one obtained by plugging the asymptotic expansion of the self-energy, Eq. (64), into Eq. (56). In the symmetry-breaking case, for any $n \in \mathbb{N}^*$, the n^{th} moment of the spectral function is related to the moments of the width according to

$$m_n = \sum_{p=1}^n \sum_{\substack{k_1 + \dots + k_p = n \\ k_1, \dots, k_p \in \mathbb{N}^*}} s_{k_1-2} \dots s_{k_p-2} , \quad (75)$$

where the inner sum runs over ordered partitions of n , and the tensor s_{-1} is defined, for convenience, as

$$s_{-1} \equiv U + \Sigma^\infty . \quad (76)$$

Let us stress that tensors s_k do not commute in general.

We provide two examples of these relations. The first moment of the spectral function equals s_{-1} ,

$$m_1 = s_{-1} = U + \Sigma^\infty . \quad (77)$$

The second moment, in contrast, involves an energy integral over Γ and reads

$$m_2 = (U + \Sigma^\infty)^2 + \int_{-\infty}^{+\infty} \frac{d\omega}{2\pi} \Gamma(\omega) . \quad (78)$$

We note that, when no symmetries are broken, we recover the relations given in Ref. [53].

The sum rules given in Eq. (75) are of importance both for the physical insight they provide and for their usefulness in numerical implementations of SCGF calculations. The 0th moment of $S(\omega)$ is, essentially, a normalisation condition. In practice, this normalisation condition can be used to perform a quasiparticle-background separation of the spectral function, so that quasiparticle resonances are separately and carefully handled [54]. The 1st moment, m_1 in Eq. (77), defines, through its eigenvalues, the effective single-particle energies (ESPEs) introduced by French and Baranger [55, 56]. ESPEs have been shown to be scale-dependent, thus hampering their traditional interpretation in terms of nuclear shells [57, 58]. Still, they provide an insightful approximate static picture of nuclei at a fixed resolution scale. The 2nd moment, m_2 in Eq. (78), characterises, after subtraction of the static part, the integrated fragmentation around the quasiparticle resonances [59]. The verification of the sum rules (75) in SCGF numerical implementations provide a good test of the numerical accuracy and consistency regarding both the static and the dynamical part of the self-energy [60]. For example, in zero-temperature calculations, one finds that the dominant features of the spectral function converge quickly with respect to reproducing its lowest moments, m_n [29].

In practical applications, this fact enables devising optimised simplifications of dressed propagators [61] and exploiting Krylov subspace projection methods [29, 62], both being crucial to converge large scale computations of medium-mass isotopes. More generally, the connection with the high-energy asymptotic expansion of the propagator, Eq. (34), indicates that a good convergence of the first moments is essential to ensure the reproduction of the high-energy behaviour of the propagator.

2. Direct relation

Using the Nambu-covariant formalism, we can also derive a direct, formal relation between the $S(\omega)$ and $\Gamma(\omega)$ tensors. Using Eqs. (23), (56) and (63), we have

$$S(\omega) = i \left((\omega + i\eta) - U - \Sigma^\infty - \int_{-\infty}^{+\infty} \frac{d\omega'}{2\pi} \frac{\Gamma(\omega')}{\omega + i\eta - \omega'} \right)^{-1} - i \left((\omega - i\eta) - U - \Sigma^\infty - \int_{-\infty}^{+\infty} \frac{d\omega'}{2\pi} \frac{\Gamma(\omega')}{\omega - i\eta - \omega'} \right)^{-1}. \quad (79)$$

Using the common Hermitian part of the advanced and retarded self-energy components, $R(\omega)$ in Eq. (70), as well as the dispersion relations, we can conveniently rewrite

$$S(\omega) = \left[\Gamma(\omega) + 2(\omega - U - R(\omega)) \Theta(\omega) \right] \left[\left((\omega - U - R(\omega))^2 + \left(\frac{\Gamma(\omega)}{2} \right)^2 \right) \left(1 + \Theta^2(\omega) \right) \right]^{-1}. \quad (84)$$

Eq. (82) is often interpreted in terms of sharp quasiparticle resonances embedded in a smooth background [51, 63, 64]. In the symmetry-conserving case, it is common to analyse the spectral function in different approximations. We concentrate on two possibilities. The first one, the so-called *peak approximation*, assumes that the spectral function has a single quasiparticle peak at a real energy $\omega = \omega_{\text{qp}}$, and discards the dispersive energy dependence of R and Γ around ω_{qp} . The second approximation, the *quasiparticle approximation*, assumes the propagator has a simple isolated pole in the complex energy plane, z_{qp} , and derives an approximated spectral function taking into account the soft energy dependence of R and Γ around the peak. These two standard analyses lead to *Lorentzian*

the previous expression as

$$S(\omega) = i \left(\omega - U - R(\omega) + i \frac{\Gamma(\omega)}{2} \right)^{-1} - i \left(\omega - U - R(\omega) - i \frac{\Gamma(\omega)}{2} \right)^{-1}. \quad (80)$$

At this stage, one typically assumes that the tensors $U + R(\omega)$ and $\Gamma(\omega)$ are simultaneously diagonalisable (see, for example, Chap. 14 of [51]) so that their commutator vanishes:

$$[U + R(\omega), \Gamma(\omega)] = 0, \quad (81)$$

where the bracket $[\cdot, \cdot]$ denotes the standard commutator. Eq. (81) is equivalent to assuming that $U + \Sigma^{R/A}(\omega)$ is normal, which, itself, is equivalent to assuming that its eigenbasis is orthogonal. In this special case, we recover the well-known formula

$$S(\omega) = \frac{\Gamma(\omega)}{(\omega - U - R(\omega))^2 + \left(\frac{\Gamma(\omega)}{2} \right)^2}. \quad (82)$$

The commuting hypothesis in Eq. (81) is, however, not necessarily fulfilled in the symmetry-broken case. We introduce the auxiliary *line-shape tensor*

$$\Theta(\omega) \equiv \left((\omega - U - R(\omega))^2 + \left(\frac{\Gamma(\omega)}{2} \right)^2 \right)^{-1} \times \left[U + R(\omega), \frac{\Gamma(\omega)}{2} \right], \quad (83)$$

which involves the commutator in Eq. (81). This tensor is in general non-zero and allows us to easily generalise Eq. (82) to the non-commutative case:

shapes, and motivate the interpretation of $U + R(\omega_{\text{qp}})$ and $\Gamma(\omega_{\text{qp}})$ as tensors characterising, respectively, the position and the width of Lorentzian resonances associated to quasiparticle states. These resonances are embedded in a smooth background associated to a residual medium, which accounts for the strength that is not concentrated on the quasiparticle peaks. Physically, the position and width of these Lorentzian-like resonances are related, respectively, to the energy and life-time of the *damped propagation* of quasiparticle states in the residual medium [65]. Together, the quasiparticle resonances and background make up the spectral function, $S(\omega)$.

We reproduce in App. C an equivalent analysis for the generalisation of the spectral function, Eq. (84). We work

out both the peak and the quasiparticle approximations. Instead of the Lorentzian resonance line-shape, characteristic of the symmetry-conserving case, we find that, in general, the resonant part of the spectral function is best described by a *Fano line-shape* [66]. In the peak approximation, there is a clear analogy between the Fano line-shape parameter, q , and the inverse of the tensor $\Theta(\omega_{\text{qp}})$. We use this analogy to provide a physical interpretation for the line-shape tensor, $\Theta(\omega)$, which we regard as describing the additional effect of *interferences* between the damped propagation of quasiparticle states in the residual medium and the excitation of a continuum of non-resonant modes displayed by the residual medium. The Fano resonances have their line-shape controlled by $\Theta^{-1}(\omega_{\text{qp}})$, whereas their positions and widths are still dictated by $U + R(\omega_{\text{qp}})$ and $\Gamma(\omega_{\text{qp}})$, respectively. In the case where the line-shape tensor is vanishingly small, we recover the standard Lorentzian picture. A similar conclusion is drawn in the quasiparticle approximation, providing further support for our interpretation.

Let us stress that the line-shape tensor $\Theta(\omega)$ vanishes in any mean-field approximation, where $\Gamma(\omega) = 0$, and in any symmetry-conserving approximation, where $U + R(\omega)$ and $\Gamma(\omega)$ are simultaneously diagonal and, hence, commute. As a consequence, one can take the line-shape tensor $\Theta(\omega)$ as a theoretical indicator of the *combined* importance of correlations and symmetry-breaking. In analogy to three-point mass differences, which can be used to probe the importance of pairing gaps, relating $\Theta(\omega)$ to a physical observable could help us find quantitative measures to detect whether a physical system is in a phase where both symmetry-breaking and correlation effects are important. This effort lies beyond the remit of our initial work.

D. Self-consistent schemes

Let us define $\mathcal{G}^{\text{Dyson}}[\Sigma]$ as the solution of the Dyson-Schwinger equation, Eq. (54), for a given self-energy Σ . Any SCGF approximation relies on approximating the exact self-energy by another functional, $\Sigma^{\text{approx}}[\mathcal{G}]$. Combined with the Dyson-Schwinger equation, the self-consistent propagator and self-energy are thus defined as the solutions $(\mathcal{G}^{\text{SC}}, \Sigma^{\text{SC}})$ of

$$\begin{pmatrix} \mathcal{G}^{\text{Dyson}}[\Sigma^{\text{SC}}] \\ \Sigma^{\text{approx}}[\mathcal{G}^{\text{SC}}] \end{pmatrix} = \begin{pmatrix} \mathcal{G}^{\text{SC}} \\ \Sigma^{\text{SC}} \end{pmatrix}. \quad (85)$$

A self-consistent scheme aims at solving Eq. (85) by iteration from a certain initial guess, until convergence to a fixed point is reached. Secs. III A, III B and III C were focused on studying $\mathcal{G}^{\text{Dyson}}[\Sigma]$ and its consequences. We now discuss a class of approximations defined by a functional $\Sigma^{\text{approx}}[\mathcal{G}]$ such that the Nambu tensor character of the self-energy is preserved. From now on, we refer to such self-consistent approximations as NC-SCGF approximations. A general self-consistent cycle is given by the diagram in Fig. 2.

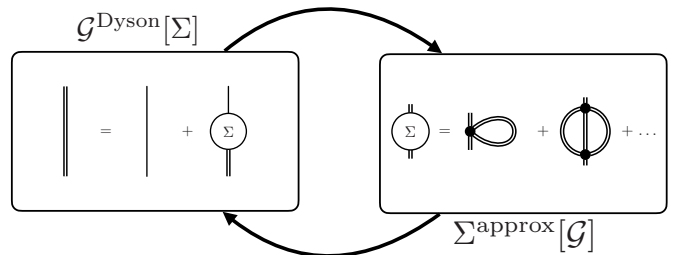


FIG. 2. Flowchart representing the self-consistent cycle solved by iterating $\mathcal{G}^{\text{Dyson}}[\Sigma]$ and $\Sigma^{\text{approx}}[\mathcal{G}]$.

Let us discuss first the exact case. The complete self-energy can be expressed as an infinite sum of Feynman diagrams derived from NCPT, as detailed in Part I. The exact (contravariant) propagator then reads

$$-\mathcal{G}^{\mu\nu}(\omega_p) = \sum_{\mathcal{G} \in \mathcal{S}} \mathcal{A}^{\mu\nu}[\mathcal{G}^{(0)}](\omega_p), \quad (86)$$

where $\mathcal{A}^{\mu\nu}[\mathcal{G}^{(0)}](\omega_p)$ denotes the amplitude associated to a diagram, \mathcal{G} , where each fermion line corresponds to an unperturbed propagator, $\mathcal{G}^{(0)}$; μ, ν are the external global indices; and ω_p is the external Matsubara frequency. For the exact case, the sum runs over the complete set of Feynman diagrams with two external lines, which we denote by \mathcal{S} . Combining Eq. (86) with the Dyson-Schwinger equation, the exact (covariant) self-energy is expressed also in terms of Feynman diagrams,

$$-\Sigma_{\mu\nu}(\omega_p) = \sum_{\mathcal{G} \in \mathcal{S}'_{1\text{PI}}} \mathcal{A}_{\mu\nu}[\mathcal{G}^{(0)}](\omega_p), \quad (87)$$

with $\mathcal{S}'_{1\text{PI}}$ the complete set of one-particle irreducible (1PI) Feynman diagrams with two amputated external lines. In other words, just as in the symmetry-conserving case, the Dyson-Schwinger equation allows us to reduce the number of diagrams. With the Dyson-Schwinger equation, we go from the complete set \mathcal{S} of diagrams for the one-body Green's functions, to the 1PI subset $\mathcal{S}'_{1\text{PI}}$ for the self-energy.

Equation (87) allows us to define approximations of the self-energy by specifying a finite subset of Feynman diagrams, $\mathcal{S}'_{\text{approx}} \subseteq \mathcal{S}'_{1\text{PI}}$. Such approximations depend on the unperturbed propagator, $\mathcal{G}^{(0)}$, through the diagrammatic expressions in Eq. (87). To build a NC-SCGF approximation, the self-energy is instead expressed directly in terms of diagrams where lines correspond to exact propagators, \mathcal{G} . This so-called *dressings* of propagator lines should help to account for correlations by incorporating medium effects into the propagator. Similarly to the symmetry-conserving case [21, 50], we avoid double-counting of NCPT diagrams by restricting the sum to the subset \mathcal{S}'_{SK} of skeleton (SK) diagrams with two amputated external lines. By definition, a Feynman

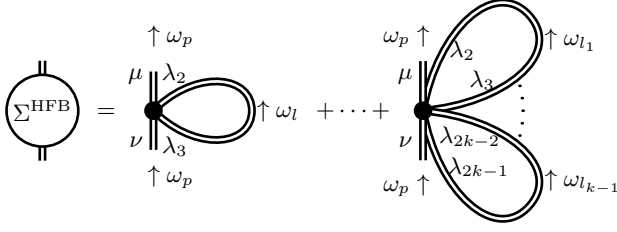


FIG. 3. Labeled diagrams contributing to the HFB self-energy with 2- up to k -body interactions. The orientation convention for the energy flow is made explicit. Double lines denote self-consistent propagators. Amputated external lines are shown, for clarity, as shortened double lines.

diagram is said to be of skeleton type if it does not contain any self-energy insertion. The self-energy can then be expressed as the sum

$$-\Sigma_{\mu\nu}(\omega_p) = \sum_{\mathcal{G} \in \mathcal{S}'_{SK}} \mathcal{A}_{\mu\nu}[\mathcal{G}](\omega_p). \quad (88)$$

We note that the amplitudes $\mathcal{A}_{\mu\nu}$ are now functionals of the fully dressed propagator, \mathcal{G} , as opposed to the unperturbed propagator, $\mathcal{G}^{(0)}$. Eq. (88) allows us to specify NC-SCGF approximations to the self-energy defined by a finite subset of Feynman diagrams, $\mathcal{S}'_{\text{approx}} \subseteq \mathcal{S}'_{SK}$. Such a self-consistent approximation amounts to summing an infinite subset of Feynman diagrams in terms of the unperturbed propagator, thus going beyond standard perturbation theory. For the case of symmetry-conserving theories, Refs. [38, 67] discussed how the self-consistency requirement implies thermodynamic consistency and the satisfaction of the conservation laws associated with symmetries of the Hamiltonian. Note that the number of skeleton diagrams can be further reduced to those containing effective interactions whenever many-body forces are present [50].

E. Hartree-Fock-Bogoliubov approximation

Let us now discuss a simple example of NC-SCGF approximation, based on a first-order expansion of the self-energy. We shall see that this gives rise to the traditional Hartree-Fock-Bogoliubov (HFB) approximation. To be specific, we approximate the self-energy by Feynman diagrams containing at most one vertex from 2-up to k -body interactions. The associated diagrams are shown in Fig. 3. In this approximation, the self-energy is energy-independent and reads, as a function of the

dressed propagator, \mathcal{G} ,

$$\Sigma_{\mu\nu}^{\text{approx}}[\mathcal{G}] = \sum_{k=2}^{k_{\text{max}}} \left[\frac{1}{2^{k-1}(k-1)!} \sum_{\lambda_2 \dots \lambda_{2k-1}} v_{[\mu \lambda_2 \lambda_3 \lambda_4 \lambda_5 \dots \nu]}^{(k)} \times \prod_{j=1}^{k-1} \frac{1}{\beta} \sum_{\omega_{l_j}} \mathcal{G}^{\lambda_{2j} \lambda_{2j+1}}(\omega_{l_j}) e^{-i\omega_{l_j} \eta_j} \right]. \quad (89)$$

We refer the reader to Part I for the Feynman rules and for more details on the notation convention, including the partial antisymmetrisation of vertices denoted by dotted indices. We obtain an equivalent equation in terms of the spectral function of the propagator by explicitly summing over Matsubara frequencies. The approximated self-energy reads, for a general spectral function, S ,

$$\Sigma_{\mu\nu}^{\text{approx}}[S] = \sum_{k=2}^{k_{\text{max}}} \left[\frac{1}{2^{k-1}(k-1)!} \sum_{\lambda_2 \dots \lambda_{2k-1}} v_{[\mu \lambda_2 \lambda_3 \lambda_4 \lambda_5 \dots \nu]}^{(k)} \times \prod_{j=1}^{k-1} \int_{-\infty}^{+\infty} \frac{d\omega_j}{2\pi} f(-\omega_j) S^{\lambda_{2j} \lambda_{2j+1}}(\omega_j) \right]. \quad (90)$$

Since the approximation of the HFB self-energy is particularly simple, we can also derive a convenient implicit equation, where the propagator is altogether removed from the equation. This is achieved by using the Dyson-Schwinger equation, Eq. (56). Since the self-energy is energy independent, Matsubara sums can be straightforwardly performed and we obtain

$$\Sigma_{\mu\nu}^{\text{HFB}} = \sum_{k=2}^{k_{\text{max}}} \left[\frac{1}{2^{k-1}(k-1)!} \sum_{\lambda_2 \dots \lambda_{2k-1}} v_{[\mu \lambda_2 \lambda_3 \lambda_4 \lambda_5 \dots \nu]}^{(k)} \times \prod_{j=1}^{k-1} f(-(U + \Sigma^{\text{HFB}}))^{\lambda_{2j} \lambda_{2j+1}} \right], \quad (91)$$

where the Fermi-Dirac distribution, $f(\omega)$, is extended into a tensor function as defined in App. B.

A key advantage of the Nambu-covariant formalism arises from the simplicity of the associated expressions. For the $k_{\text{max}} = 2$ case, for instance, the implicit equation Eq. (91) involves the contraction of a two-body matrix element with a Fermi-Dirac distribution evaluated at the quasiparticle (tensor) energy $\omega = -(U + \Sigma^{\text{HFB}})$. Eq. (91) is deceptively close to the expression of the symmetry-conserving (self-consistent) Hartree-Fock approximation [49]. We stress, however, that this expression incorporates all the complexity of the symmetry-broken case.

We also want to stress that Eq. (91) generalises straightforwardly the standard HFB equations to the case of interactions with $k > 2$. For nuclear physics applications, three-body interactions ($k = 3$) are relevant. The

HFB contribution of three-body interactions arises, as expected, as a double fermion contraction over a partially antisymmetrised three-body interaction. In numerical terms, we stress that the partial antisymmetrisation of two- or three-body interactions does not contribute to the self-consistent cycle and can thus be factorised as a one-off pre-computing step. One can then iterate the self-consistent cycle until convergence is reached. Having determined Σ^{HFB} , one can immediately obtain the propagator via Eq. (56) and, in turn, the ground-state energy of the system through the GMK sum rule.

At this point, we have discussed the lowest-order self-consistent approximation to the self-energy. NC-SCGF approximations of the self-energy can be refined by adding more and more Feynman diagrams, combined with self-consistently dressed propagators. One could do this, for instance, by considering the second- and third-order NCPT diagrams, of skeleton type, given in Part I and dressing the corresponding lines. To go beyond any finite order SCGF approximation, several approaches have been proposed. For example, the algebraic diagrammatic construction has been applied to devise approximations summing ladder and rings diagram at zero-temperature in the symmetry-conserving case [24, 68]. Instead, we follow here a more versatile approach. We go beyond any finite order NC-SCGF approximation by dressing self-consistently not only the fermion lines, but also the interaction vertices.

IV. SELF-CONSISTENT INTERACTIONS

In this section, we discuss the self-consistent procedure associated to the dressing of vertices in a Nambu-covariant formalism. First, we derive the full equations of motion for the one-body Green's function. This allows us to formulate NC-SCGF schemes as approximations of exact many-body vertices. Second, we discuss the self-consistent dressing of a two-body interaction via a Bethe-Salpeter equation [41] in Sec. IV B. Last, we work out explicitly the example of the ladder dressing of the two-body interaction in Sec. IV C. We stress that we only discuss specific examples of self-consistent interactions. For a more general discussion on self-consistent vertices, we refer the reader to Refs. [69, 70], where they are introduced by means of a Legendre transformations and related to a diagrammatic expansion.

A. Equations of motion

Solving the A-body problem for a given physical system is equivalent to computing all k -body Green's functions associated to the Hamiltonian Ω describing the physical system. The different k -body Green's functions are, however, not independent from one another. The relations between different k -body Green's functions take the form of a hierarchy of equations of motion derived originally by Kadanoff, Martin and Schwinger (KMS) [44, 71, 72].

For simplicity we focus in this section on the equation of motion coupling the one-body to higher k -body Green's functions through generic $v^{(k)}$ interaction terms.

1. Equation of motion of the propagator

We now proceed to derive the equations of motion for the one-body Green's function, i.e. the propagator. We work with the Hamiltonian partitioning described in Eqs. (52). We start by considering the equation of motion of a simple Nambu field,

$$\partial_\tau A^\mu(\tau) = [\Omega, A^\mu(\tau)] , \quad (92)$$

with τ an imaginary time. Using Eq. (8a), the equation of motion for the propagator reads

$$-\partial_\tau \mathcal{G}^{\mu\nu}(\tau, \tau') = \delta(\tau - \tau') g^{\mu\nu} + \langle \text{T} [[\Omega, A^\mu(\tau)] A^\nu(\tau')] \rangle . \quad (93)$$

To compute the commutator in the right hand side of the previous expression, we use its derivation property, namely,

$$\left[\prod_{j=1}^{2k} A^{\mu_j}, A^\mu \right] = \sum_{i=1}^{2k} (-1)^i g^{\mu_i \mu} \prod_{\substack{j=1 \\ j \neq i}}^{2k} A^{\mu_j} , \quad (94)$$

where the products are to be written from left to right with increasing j . With this, the equation of motion is seen to couple the one-body Green's function to higher k -body Green's functions,

$$\begin{aligned} \sum_{\mu_1} (-g^{\mu_1 \mu} \partial_\tau - U^{\mu_1 \mu}) \mathcal{G}^{\mu_1 \nu}(\tau, \tau') &= \delta(\tau - \tau') g^{\mu\nu} \\ &- \sum_{k=1}^{k_{\max}} \frac{(-1)^k}{(2k-1)!} \sum_{\alpha \mu_1 \dots \mu_{2k-1}} g^{\alpha \mu} v_{[\alpha \mu_1 \dots \mu_{2k-1}] }^{(k)} \\ &\quad \times \mathcal{G}^{\mu_1 \dots \mu_{2k-1} \nu}(\tau, \tau') , \end{aligned} \quad (95)$$

where U is the traceless antisymmetric tensor associated to the unperturbed Hamiltonian, Eq. (52b). Further, we use the notation $\mathcal{G}^{\mu_1 \dots \mu_{2k}}(\tau, \tau')$ to denote the time limit

$$\begin{aligned} &(-1)^k \mathcal{G}^{\mu_1 \dots \mu_{2k}}(\tau, \tau') \\ &\equiv \langle \text{T} [A^{\mu_1}(\tau^+ \dots \tau^+) \dots A^{\mu_{2k-1}}(\tau^+) A^{\mu_{2k}}(\tau')] \rangle \\ &\equiv \lim_{\tau_1 > \dots > \tau_{2k-1} \rightarrow \tau^+} (-1)^k \mathcal{G}^{\mu_1 \dots \mu_{2k}}(\tau_1, \dots, \tau_{2k-1}, \tau') . \end{aligned} \quad (96)$$

We also use the notation defined in Eq. (38) to denote a partially antisymmetric part of $v^{(k)}$.

To express Eq. (95) in terms of k -body Green's functions and of the self-energy, we contract it with the unperturbed propagator $\mathcal{G}^{(0)}$ and integrate over time to

FIG. 4. Diagrammatic representation of Eq. (99).

find

$$\begin{aligned} \mathcal{G}^{\mu\nu}(\tau, \tau') &= \mathcal{G}^{(0)\mu\nu}(\tau, \tau') \\ &- \sum_{k=1}^{k_{\max}} \frac{(-1)^k}{(2k-1)!} \sum_{\mu_1 \dots \mu_{2k}} \int_0^\beta ds \mathcal{G}^{(0)\mu\mu_1}(\tau, s) v_{[\mu_1 \dot{\mu}_2 \dots \dot{\mu}_{2k}]}^{(k)} \\ &\quad \times \mathcal{G}^{\mu_2 \dots \mu_{2k}\nu}(s, \tau'). \end{aligned} \quad (97)$$

Note that the right-hand-side couples the propagator to all k -body Green's functions via the k -body interaction. In the case where $k_{\max} = 2$, the equation couples the one- and the two-body Green's functions. This is equivalent to the first equation of KMS hierarchy.

The general equation can be further simplified by using the Dyson-Schwinger equation, Eq. (59), to find

$$\begin{aligned} &\sum_{\mu_1} \int_0^\beta ds \Sigma_{\mu\mu_1}(\tau, s) \mathcal{G}^{\mu_1\nu}(s, \tau') \\ &= - \sum_{k=1}^{k_{\max}} \frac{(-1)^k}{(2k-1)!} \sum_{\mu_2 \dots \mu_{2k}} v_{[\mu \dot{\mu}_2 \dots \dot{\mu}_{2k}]}^{(k)} \mathcal{G}^{\mu_2 \dots \mu_{2k}\nu}(\tau, \tau'). \end{aligned} \quad (98)$$

With Eq. (98), we have a relation between the one-body Green's function, the self-energy and higher-order Green's functions. Instead of defining a NC-SCGF approximation at the level of the self-energy, we can design NC-SCGF approximations from diagrammatic truncations of (higher) k -body Green's functions. These truncations are then brought back to approximations on the self-energy using Eq. (98). Shifting our focus to higher k -body Green's functions will allow us to easily design richer many-body approximations that incorporate self-consistent interactions. To do this, however, we first need to introduce the exact many-body interaction vertices on which these approximations are based. Ultimately, we will be able to rewrite Eq. (98) in terms of such self-consistent interaction vertices, rather than the associated k -body Green's functions.

2. Exact many-body vertices

We define exact many-body vertices as the amputated connected part of the corresponding many-body Green's function. For example, the exact two-body vertex $\Gamma_{\mu_1 \mu_2 \mu_3 \mu_4}^{(2)}(\tau_1, \tau_2, \tau_3, \tau_4)$ is defined implicitly by the

FIG. 5. Diagrammatic representation of Eq. (102).

following equation,

$$\begin{aligned} \mathcal{G}^{\mu_1 \mu_2 \mu_3 \mu_4}(\tau_1, \tau_2, \tau_3, \tau_4) &\equiv \mathcal{G}^{\mu_1 \mu_4}(\tau_1, \tau_4) \mathcal{G}^{\mu_2 \mu_3}(\tau_2, \tau_3) \\ &- \mathcal{G}^{\mu_1 \mu_3}(\tau_1, \tau_3) \mathcal{G}^{\mu_2 \mu_4}(\tau_2, \tau_4) + \mathcal{G}^{\mu_1 \mu_2}(\tau_1, \tau_2) \mathcal{G}^{\mu_3 \mu_4}(\tau_3, \tau_4) \\ &- \sum_{\lambda_1 \lambda_2 \lambda_3 \lambda_4} \int_0^\beta d\tau'_1 d\tau'_2 d\tau'_3 d\tau'_4 \mathcal{G}^{\mu_1 \lambda_1}(\tau_1, \tau'_1) \mathcal{G}^{\mu_2 \lambda_2}(\tau_2, \tau'_2) \\ &\times \Gamma_{\lambda_1 \lambda_2 \lambda_3 \lambda_4}^{(2)}(\tau'_1, \tau'_2, \tau'_3, \tau'_4) \times \mathcal{G}^{\lambda_4 \mu_4}(\tau'_4, \tau_4) \mathcal{G}^{\lambda_3 \mu_3}(\tau'_3, \tau_3), \end{aligned} \quad (99)$$

involving exact one- and two-body propagators, $\mathcal{G}^{\mu_1 \mu_2}$ and $\mathcal{G}^{\mu_1 \mu_2 \mu_3 \mu_4}$, respectively. For a diagrammatic representation of Eq. (99), see Fig. 4. The exact two-body vertex is clearly the remaining diagrammatic component after all disconnected contributions to $\mathcal{G}^{\mu_1 \mu_2 \mu_3 \mu_4}$ have been eliminated.

For simplicity, we consider from now on the case where the perturbative part of the Hamiltonian contains only a two-body interaction. In other words, we assume that $k_{\max} = 2$ and $v_{\mu_1 \mu_2}^{(1)} = v^{(0)} = 0$. With this, the partitioning of Eqs. (52) remains unchanged but the perturbative part of Eq. (52c) becomes

$$\Omega_1 \equiv \frac{1}{4!} \sum_{\mu_1 \mu_2 \mu_3 \mu_4} v_{\mu_1 \mu_2 \mu_3 \mu_4}^{(2)} A^{\mu_1} A^{\mu_2} A^{\mu_3} A^{\mu_4}. \quad (100)$$

In this case, the one-body Green's function couples only to the two-body Green's function through the equation of motion, Eq. (95). Therefore, the relation between the self-energy and the two-body Green's function reads simply

$$\begin{aligned} &\sum_{\mu_1} \int_0^\beta ds \Sigma_{\mu\mu_1}(\tau, s) \mathcal{G}^{\mu_1\nu}(s, \tau') \\ &= - \frac{1}{3!} \sum_{\mu_2 \mu_3 \mu_4} v_{[\mu \dot{\mu}_2 \dot{\mu}_3 \dot{\mu}_4]}^{(2)} \mathcal{G}^{\mu_2 \mu_3 \mu_4 \nu}(\tau^{+++}, \tau^{++}, \tau^+, \tau'), \end{aligned} \quad (101)$$

where all the time variables in the two-body Green's function are written explicitly for clarity. Using the implicit definition of $\Gamma^{(2)}$, Eq. (99), the equation of motion is expressed as a relation between the self-energy, Σ , and

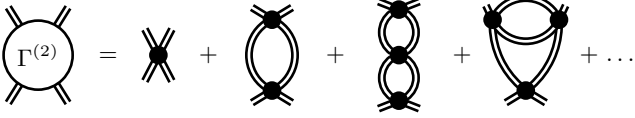


FIG. 6. Diagrammatic content of the exact two-body vertex up to third order. We omit amputated diagrams which are equivalent up to a permutation of the external legs for the sake of conciseness.

the exact two-body vertex, $\Gamma^{(2)}$,

$$\begin{aligned}
 -\Sigma_{\mu\nu}(\tau, \tau') &= \frac{1}{2} \sum_{\lambda_1 \lambda_2} v_{[\mu\lambda_1\lambda_2\nu]}^{(2)} \delta(\tau - \tau') \mathcal{G}^{\lambda_1\lambda_2}(\tau^+, \tau) \\
 &- \frac{1}{3!} \sum_{\substack{\lambda_1\lambda_2\lambda_3 \\ \lambda'_1\lambda'_2\lambda'_3}} v_{[\mu\lambda_1\lambda_2\lambda_3]}^{(2)} \int_0^\beta d\tau'_1 d\tau'_2 d\tau'_3 \Gamma_{\lambda'_3\lambda'_2\lambda'_1\nu}^{(2)}(\tau'_3, \tau'_2, \tau'_1, \tau') \\
 &\quad \times \mathcal{G}^{\lambda_1\lambda'_1}(\tau, \tau'_1) \mathcal{G}^{\lambda_2\lambda'_2}(\tau, \tau'_2) \mathcal{G}^{\lambda_3\lambda'_3}(\tau, \tau'_3). \quad (102)
 \end{aligned}$$

We note that, remarkably, the totally and partially anti-symmetric vertices defined in the NCPT of Part I appear here but, this time, on the pure basis of non-perturbative arguments. The same remark applies to the symmetry factors. Hence, $\Gamma^{(2)}$ can be understood as the kernel for any self-energy contributions that go beyond the contribution associated to the HFB diagram. Eq. (102) is represented diagrammatically in Fig. 5.

Now that we have a relation between the exact two-body vertex, $\Gamma^{(2)}$, and the self-energy, Σ , we turn to discuss the dependence of $\Gamma^{(2)}$ on the dressed propagator, \mathcal{G} . We express the exact two-body vertex in terms of Feynman diagrams with dressed propagators,

$$\begin{aligned}
 \Gamma_{\mu_1\mu_2\mu_3\mu_4}^{(2)}(\tau_1, \tau_2, \tau_3, \tau_4) &\equiv \\
 &\sum_{\mathcal{G} \in \mathcal{T}'_{SK}} \mathcal{A}_{\mu_1\mu_2\mu_3\mu_4}[\mathcal{G}](\tau_1, \tau_2, \tau_3, \tau_4). \quad (103)
 \end{aligned}$$

Here, \mathcal{T}'_{SK} represents the set of skeleton Feynman diagrams with four amputated external lines. $\mathcal{A}_{\mu_1\mu_2\mu_3\mu_4}[\mathcal{G}](\tau_1, \tau_2, \tau_3, \tau_4)$ are the associated amplitudes for a given dressed propagator, \mathcal{G} . These amplitudes can be obtained using the Feynman rules described in Part I. We show Feynman diagrams up to third order in the interaction vertex in Fig. 6. We have omitted diagrams that are equivalent up to a permutation of the amputated lines. Those must be included explicitly in Eq. (103)⁹.

In the two-body interaction case, the self-energy depends only on \mathcal{G} and $\Gamma^{(2)}$ via Eq. (102). We denote this

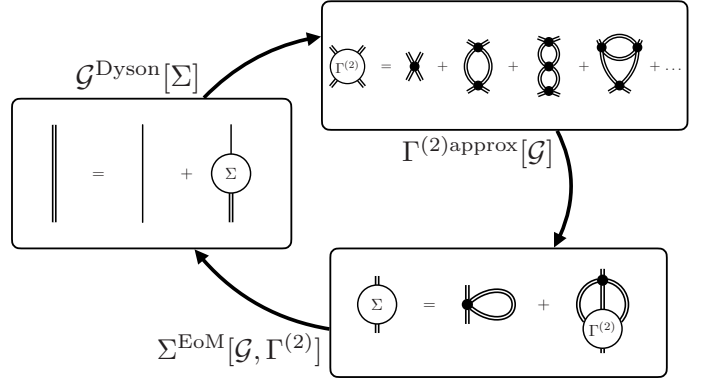


FIG. 7. Flowchart representing the self-consistent cycle solved by iterating $\mathcal{G}^{\text{Dyson}}[\Sigma]$, $\Sigma^{\text{EoM}}[\mathcal{G}, \Gamma^{(2)}]$ and $\Gamma^{(2)\text{approx}}[\mathcal{G}]$.

self-energy as $\Sigma^{\text{EoM}}[\mathcal{G}, \Gamma^{(2)}]$. The self-consistent scheme summarised in Eq. (85) can be reformulated in terms of approximated many-body vertices. In this formulation, we look for the solutions ($\mathcal{G}^{\text{SC}}, \Sigma^{\text{SC}}, \Gamma^{(2)\text{SC}}$) of

$$\begin{pmatrix} \mathcal{G}^{\text{Dyson}}[\Sigma^{\text{SC}}] \\ \Sigma^{\text{EoM}}[\mathcal{G}^{\text{SC}}, \Gamma^{(2)\text{SC}}] \\ \Gamma^{(2)\text{approx}}[\mathcal{G}^{\text{SC}}] \end{pmatrix} = \begin{pmatrix} \mathcal{G}^{\text{SC}} \\ \Sigma^{\text{SC}} \\ \Gamma^{(2)\text{SC}} \end{pmatrix}, \quad (104)$$

where $\Gamma^{(2)\text{approx}}[\mathcal{G}]$ denotes an approximated functional of the exact two-body vertex. This formulation of the self-consistent cycle, given by Eq. (104), is shown in terms of diagrams in the flowchart of Fig. 7. For example, $\Gamma^{(2)\text{approx}}[\mathcal{G}]$ can be any truncation on the set of Feynman diagrams contributing in Eq. (103).

Additionally, we stress that this formulation allows us to introduce approximated functionals which are self-consistent not only in the propagator, but also in the interaction vertices. This is done by choosing a functional, $\Gamma^{(2)\text{approx}}[\mathcal{G}]$, defined as a self-consistent solution in $\Gamma^{(2)}$ of an auxiliary functional, $\Gamma^{(2)\text{implicit}}[\mathcal{G}, \Gamma^{(2)}]$. We shall now work out explicitly one of these approximations and discuss in more detail the relevance of the auxiliary functional.

B. Bethe-Salpeter equation

To go beyond any finite order NC-SCGF approximation, we have introduced in Sec. IV A approximations on the exact two-body vertex defined by an auxiliary functional, $\Gamma^{(2)\text{implicit}}[\mathcal{G}, \Gamma^{(2)}]$. A specific approximated functional is typically chosen depending on the many-body system under study and on the available computational resources. In this section, we introduce a class of functionals based on a Bethe-Salpeter equation satisfied by the exact two-body vertex.

⁹ Alternatively, we could consider only one diagram per class of equivalence and perform an *ad hoc* antisymmetrisation procedure.

1. Motivations

The general rationale underlying the Bethe-Salpeter equation [41] is similar to the one motivating the Dyson-Schwinger equation. In the case of the Dyson-Schwinger equation, we require that the poles in energy of the unperturbed one-body Green's function *must* be shifted in order to achieve a precise enough approximation. However, for any correction made of a finite number of Feynman diagrams, the poles from the unperturbed part of the propagator remain un-modified¹⁰. To design approximations that can shift unperturbed poles, the self-energy and, correspondingly, the Dyson-Schwinger equation are introduced. With this, any finite number of 1PI Feynman diagrams contributing to the self-energy will generate, through the Dyson-Schwinger equation, an infinite number of Feynman diagrams contributing to the one-body Green's function, shifting its poles accordingly. The HFB approximation of the self-energy is a classical example of this approach.

Similarly, let us assume that the poles in energy of the two-body Green's function *must* be shifted compared to those obtained by a simple product of two one-body Green's functions. An approximation based on a finite number of Feynman diagrams in $\Gamma^{(2)}$ cannot achieve this goal. To design approximations where these shifts are possible, we distinguish between *irreducible* and *reducible* contributions¹¹. For any finite number of irreducible Feynman diagrams, an infinite number of reducible diagrams are generated by iteration, so that poles of the two-body Green's function are shifted. Since the two-body Green's function depends on three independent energies, poles can be shifted in three directions. These three possibilities are reflected in three different ways of building reducible diagrams from an irreducible set. A classical example of a set of equations that relate a two-body irreducible part to reducible components is the parquet equations. For a detailed account of parquet equations in the symmetry-conserving case, we refer the reader to Chap. 15 of Ref. [51].

The parquet equations have high potentialities but, unfortunately, their application to nuclear physics has been hampered by numerical complexity. Ref. [73] describes an attempt in the symmetry-conserving case. The main difference with respect to the Dyson-Schwinger equation is that the parquet equations cannot be expressed as an explicit functional of irreducible diagrams. As a consequence, computing the infinite set of reducible diagrams contributing to $\Gamma^{(2)}$ from the parquet equations is an

iterative process, starting from a set (its kernel) of chosen irreducible diagrams. To the best of our knowledge, even in the simplest case where just one interaction vertex is used for the irreducible kernel, the numerical complexity to evaluate the whole parquet series has not yet been overcome for nuclear systems. In particular, the attempts of Ref. [73] were hindered by the uncontrolled energy behaviour near isolated poles of the propagators. Ref. [74] resolved these issues by reformulating the problem as an energy-independent eigenvalue problem. While the latter work focused on improving approximations for the Bethe-Salpeter equation, it could also resum one particular channel on the parquet equations. Further computational developments remain necessary in that direction.

An alternative option is possible. To bypass the numerical complexity of the parquet equations, the class of irreducible diagrams can be enlarged so that the reducible contributions become simpler to compute. One faces different possibilities when it comes to preselecting these contributions. In our case, we want to describe the microscopic properties and the thermodynamics of superfluid nuclear matter. We choose to keep both particle-hole ring diagrams as well as particle-particle ladder diagrams. Iterated particle-hole excitations impact non-trivially the collective behaviour of the many-body system in the low-energy and long-range regime. These correlations are known to bring important corrections in the description of, for instance, giant resonances [75, 76]. Complementarily, the sum of particle-particle ladders impacts the short-range and high-energy behaviour of the many-body system, which is relevant for the macroscopic properties of the system. The ladders corrections are necessary to properly account for the strong repulsion (or even a hard core) part of a two-body interaction [33–37]. In each one of these two cases, the generation of reducible diagrams from an irreducible set takes the form of a particular Bethe-Salpeter equation. For more details on those aspects we refer the reader to Chap. 6 of Ref. [77]. When particle-number symmetry is broken, the particle-hole and particle-particle excitations are coupled to each other. In the following, we specify the type of irreducible diagrams that we consider to address these correlations. We also discuss how a unique Bethe-Salpeter equation generates a set of reducible diagrams contributing to $\Gamma^{(2)}$, including particle-particle ladders, particle-hole rings and their coupling.

2. Bethe-Salpeter equation

We want to describe $\Gamma^{(2)}$ in terms of a Bethe-Salpeter equation, to limit the computational complexity while keeping our ability to describe the relevant phenomenology of the many-body system. We aim to generate particle-hole rings and particle-particle ladders from the Bethe-Salpeter equation starting from an irreducible set of diagrams. In the case of an S-wave contact interaction, the relevant equation was studied by Haussmann [78, 79].

¹⁰ See for instance the second- and third-order corrections to the propagator in Part I. While new poles are generated as linear combinations of single-particle energies, the poles from the original unperturbed contribution are un-affected.

¹¹ This is similar in spirit to the Dyson-Schwinger equation, where only 1PI diagrams are kept and then iterated to generate an infinite number of reducible terms.

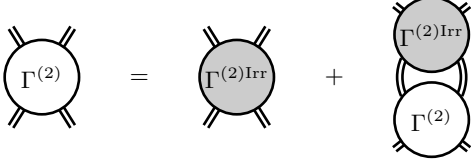


FIG. 8. Diagrammatic representation of the Bethe-Salpeter equation, Eq. (105). To easily distinguish the irreducible part, $\Gamma^{(2)\text{Irr}}$, is represented with a shaded grey background.

Similarly, we consider the following Bethe-Salpeter equation

$$\begin{aligned} \Gamma_{\mu_1\mu_2\mu_3\mu_4}^{(2)}(\tau_1, \tau_2, \tau_3, \tau_4) &= \Gamma_{\mu_1\mu_2\mu_3\mu_4}^{(2)\text{Irr}}(\tau_1, \tau_2, \tau_3, \tau_4) \\ &+ \frac{1}{2} \sum_{\substack{\lambda_1\lambda_2 \\ \lambda'_1\lambda'_2}} \int_0^\beta d\tau_{\lambda_1} d\tau_{\lambda_2} d\tau_{\lambda'_1} d\tau_{\lambda'_2} \Gamma_{\mu_1\mu_2\lambda_2\lambda_1}^{(2)\text{Irr}}(\tau_1, \tau_2, \tau_{\lambda_2}, \tau_{\lambda_1}) \\ &\times \mathcal{G}^{\lambda_1\lambda'_1}(\tau_{\lambda_1}, \tau_{\lambda'_1}) \mathcal{G}^{\lambda_2\lambda'_2}(\tau_{\lambda_2}, \tau_{\lambda'_2}) \\ &\times \Gamma_{\lambda'_1\lambda'_2\mu_3\mu_4}^{(2)}(\tau_{\lambda'_1}, \tau_{\lambda'_2}, \tau_3, \tau_4), \end{aligned} \quad (105)$$

where $\Gamma_{\mu_1\mu_2\mu_3\mu_4}^{(2)\text{Irr}}(\tau_1, \tau_2, \tau_3, \tau_4)$ denotes the sum of irreducible Feynman diagrams such that, by definition, the two-body vertex obtained by Eq. (105) is exact. Eq. (105) is represented diagrammatically in Fig. 8.

To determine the subset of diagrams that contribute to the irreducible part, let us recall that $\Gamma^{(2)}$ is the sum of dressed skeleton diagrams with four amputated external lines. Consequently, the irreducible part, $\Gamma^{(2)\text{Irr}}$, must include all necessary diagrams such that the whole set of skeleton ones are generated by iteration of the Bethe-Salpeter equation, Eq. (105). In this case, it is straightforward to show that the class of irreducible diagrams is the class of amputated dressed diagram that are both skeleton and [12]-simple. A diagram is said to be [12]-simple if, by cutting two internal lines, it cannot be separated into two disconnected parts, such that one part contains lines 1 and 2 and the other, lines 3 and 4¹². We show in Fig. 9 some examples contributing to the irreducible part of $\Gamma^{(2)}$.

The Bethe-Salpeter equation (105) defines an auxiliary functional $\Gamma^{(2)\text{Implicit-BS}}[\mathcal{G}, \Gamma^{(2)}, \Gamma^{(2)\text{Irr approx}}]$. The solution of Eq. (105), self-consistent in $\Gamma^{(2)}$, is then denoted by the functional $\Gamma^{(2)\text{BS}}[\mathcal{G}, \Gamma^{(2)\text{Irr approx}}]$. For a given approximated functional of the irreducible part $\Gamma^{(2)\text{Irr approx}}[\mathcal{G}]$, we obtain a new self-consistent cycle as shown in Fig. 10. Note that the approximated two-body vertex must be computed iteratively from $\Gamma^{(2)\text{Implicit-BS}}[\mathcal{G}, \Gamma^{(2)}, \Gamma^{(2)\text{Irr approx}}]$ which increases the numerical cost of the self-consistent

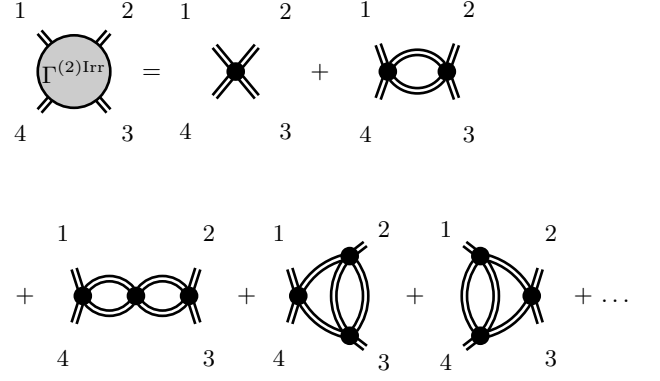


FIG. 9. Examples of amputated Feynman diagrams contributing to the irreducible part of the two-body vertex. For clarity, we write explicitly the numbers associated to each amputated external line. Two amputated diagrams differing only by a permutation of the amputated lines can also differ in their irreducible character. We do not exhaust the contributions up to third order for the sake of conciseness.

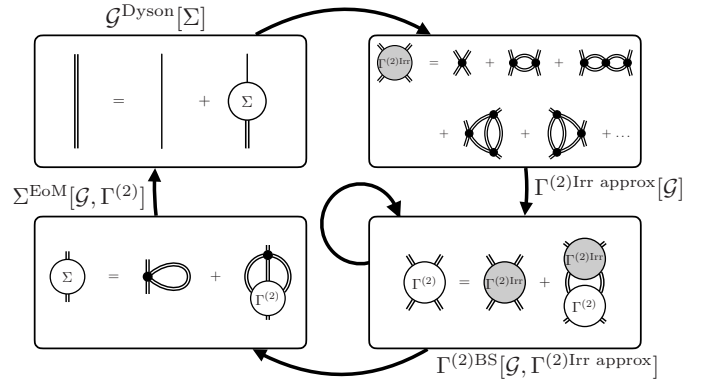


FIG. 10. Flowchart representing the self-consistent cycle obtained by iterating $\mathcal{G}^{\text{Dyson}}[\Sigma]$, $\Sigma^{\text{EoM}}[\mathcal{G}, \Gamma^{(2)}]$, $\Gamma^{(2)\text{Irr approx}}[\mathcal{G}]$ and $\Gamma^{(2)\text{BS}}[\mathcal{G}, \Gamma^{(2)\text{Irr approx}}]$. The inner cycle represents the iterations on $\Gamma^{(2)}$, which are necessary to evaluate $\Gamma^{(2)\text{BS}}[\mathcal{G}, \Gamma^{(2)\text{Irr approx}}]$ from the auxiliary functional $\Gamma^{(2)\text{Implicit-BS}}[\mathcal{G}, \Gamma^{(2)}, \Gamma^{(2)\text{Irr approx}}]$.

scheme by a non-negligible amount. As it will be shown in Sec. IV C, this extra cost can be avoided in the particular case of the *self-consistent ladder approximation* by working out an explicit functional of the propagator.

C. Ladder approximation

The ladder approximation is introduced as the first order truncation on the irreducible part of the two-body vertex in the Bethe-Salpeter equation, Eq. (105). The approximated irreducible two-body vertex is given by the

¹² By line i we mean here the line associated to the global index μ_i and imaginary-time τ_i . We follow here the definition given in Chap. 15 of Ref. [51].

first term in Fig. 9 and consequently reads

$$\Gamma_{\mu_1\mu_2\mu_3\mu_4}^{(2)\text{Irr Ladder}}(\tau_1, \tau_2, \tau_3, \tau_4) \equiv v_{[\mu_1\mu_2\mu_3\mu_4]}^{(2)} \delta(\tau_1 - \tau_2) \delta(\tau_3 - \tau_4) \delta(\tau_1 - \tau_3). \quad (106)$$

The resulting approximated two-body vertex is called (in-medium) T -matrix and denoted $T_{\mu_1\mu_2\mu_3\mu_4}(\tau_1, \tau_2, \tau_3, \tau_4)$.

In this section, we derive an implicit equation on the T -matrix. We then find an explicit functional $T[\mathcal{G}]$, so that the iterative cycle on the T -matrix is avoided. Exact properties satisfied by the T -matrix are detailed inasmuch as they allow us to express the equations of the self-consistent ladder approximation in terms of spectral functions only. In addition, we discuss the convergence of the series of ladders for a HFB propagator. We give a sufficient condition to guarantee the convergence for any Hermitian two-body interaction.

1. Implicit equation

Plugging the first-order approximation of the irreducible two-body vertex, Eq. (106), into the Bethe-Salpeter equation, Eq. (105), we see that the T -matrix only depends on two times, τ_1 and τ_4 ,

$$T_{\mu_1\mu_2\mu_3\mu_4}(\tau_1, \tau_2, \tau_3, \tau_4) = T_{\mu_1\mu_2\mu_3\mu_4}(\tau_1, \tau_4) \delta(\tau_1 - \tau_2) \delta(\tau_3 - \tau_4), \quad (107)$$

provided we factorise the two Dirac distribution on τ_2 and τ_3 . The simplified Bethe-Salpeter equation reads

$$T_{\mu_1\mu_2\mu_3\mu_4}(\tau_1, \tau_4) = v_{[\mu_1\mu_2\mu_3\mu_4]}^{(2)} \delta(\tau_1 - \tau_4) + \frac{1}{2} \sum_{\substack{\lambda_1 \lambda_2 \\ \lambda'_1 \lambda'_2}} \int_0^\beta d\tau' v_{[\mu_1\mu_2\lambda_2\lambda_1]}^{(2)} \mathcal{G}^{\lambda_1\lambda'_1}(\tau_1, \tau') \mathcal{G}^{\lambda_2\lambda'_2}(\tau_1, \tau') \times T_{\lambda'_1\lambda'_2\mu_3\mu_4}(\tau', \tau_4). \quad (108)$$

Eq. (108) is shown in Fig. 11. From Eq. (108), we can show that $(\partial_{\tau_1} + \partial_{\tau_4}) T_{\mu_1\mu_2\mu_3\mu_4}(\tau_1, \tau_4)$ satisfies an homogeneous Fredholm integral equation. Assuming the kernel to be non-singular implies that

$$(\partial_{\tau_1} + \partial_{\tau_4}) T_{\mu_1\mu_2\mu_3\mu_4}(\tau_1, \tau_4) = 0 \quad (109)$$

so that T only depends on the relative time $\tau \equiv \tau_1 - \tau_4$ and we define

$$T_{\mu_1\mu_2\mu_3\mu_4}(\tau) \equiv T_{\mu_1\mu_2\mu_3\mu_4}(\tau_1 - \tau_4, 0) = T_{\mu_1\mu_2\mu_3\mu_4}(\tau_1, \tau_4). \quad (110)$$

To further simplify the notation, we introduce the following multi-indices

$$M \equiv (\mu_1, \mu_2), \quad (111a)$$

$$N \equiv (\mu_3, \mu_4), \quad (111b)$$

$$L \equiv (\lambda_1, \lambda_2), \quad (111c)$$

$$L' \equiv (\lambda'_1, \lambda'_2), \quad (111d)$$

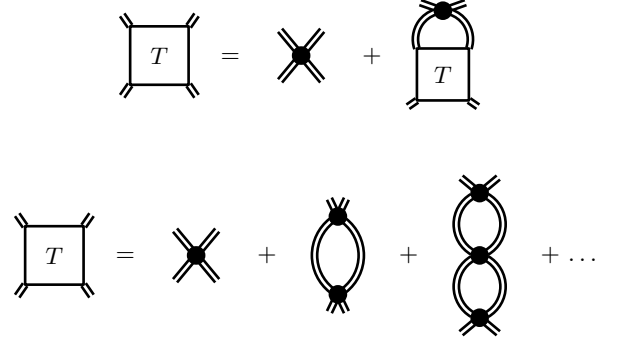


FIG. 11. Top: diagrammatic representation of the implicit equation (108) on the T -matrix. Bottom: explicit diagrammatic expression of the T -matrix. Since T has equal incoming or outgoing times, it is represented by a rectangular box.

and define the objects

$$T_{MN}(\tau) \equiv T_{\mu_1\mu_2\mu_3\mu_4}(\tau), \quad (112a)$$

$$V_{MN}^{(2)} \equiv v_{[\mu_1\mu_2\mu_3\mu_4]}^{(2)}, \quad (112b)$$

$$\Pi^{LL'}(\tau) \equiv -\mathcal{G}^{\lambda_1\lambda'_1}(\tau) \mathcal{G}^{\lambda_2\lambda'_2}(\tau). \quad (112c)$$

In keeping with the standard symmetry-conserving nomenclature, we refer to $\Pi^{LL'}(\tau)$ as the “bubble” propagator or, simply, the bubble. As with global indices, we use an intrinsic notation for the multi-indices M, N, \dots i.e. multi-indices are dropped whenever there is no ambiguity. For example, since Ω_1 is assumed to be Hermitian, the potential satisfies the symmetries

$$V^{(2)} = V^{(2)\dagger}, \quad (113a)$$

$$V^{(2)} = V^{(2)\Gamma}, \quad (113b)$$

where the Hermitian conjugation of a (p, q) -tensor is defined in App. A and where the transposition is defined for $(0, 4)$ -, $(4, 0)$ - and $(2, 2)$ -tensors respectively by

$$t_{MN}^\Gamma \equiv t_{NM}, \quad (114a)$$

$$(t^\Gamma)^{MN} \equiv t^{NM}, \quad (114b)$$

$$(t^\Gamma)^M_N \equiv (t^\Gamma)_N^M. \quad (114c)$$

With this additional notation, the Bethe-Salpeter equation reads, simply,

$$T(\tau) = V^{(2)} \delta(\tau) + \frac{1}{2} V^{(2)} \int_0^\beta d\tau' \Pi(\tau - \tau') T(\tau'). \quad (115)$$

Finally, using the β -quasiperiodicity of the propagator stated in Eq. (12b), we find that the bubble, Π , and the T -matrix, T , are β -periodic functions. Consequently, we introduce their energy representations, $\Pi(\Omega_p)$ and $T(\Omega_p)$,

using the Fourier transforms

$$\Pi(\Omega_p) \equiv \int_0^\beta d\tau e^{i\Omega_p \tau} \Pi(\tau), \quad (116)$$

$$T(\Omega_p) \equiv \int_0^\beta d\tau e^{i\Omega_p \tau} T(\tau), \quad (117)$$

where $\Omega_p \equiv 2p\frac{\pi}{\beta}$ are bosonic Matsubara frequencies. The appearance of these frequencies is a consequence of β -periodicity, but also highlights the fact that the bubble and the T -matrix are two-fermion functions. In other words, they describe (bosonic) two-fermion pair propagation and scattering in the medium. In the energy representation, the Bethe-Salpeter equation becomes

$$T(\Omega_p) = V^{(2)} + \frac{1}{2} V^{(2)} \Pi(\Omega_p) T(\Omega_p). \quad (118)$$

Comparing Eqs. (54) to Eq. (118), the similarity between the Bethe-Salpeter equation and the Dyson-Schwinger appears clearly.

2. Exact properties

The T -matrix and the bubble, Π , verify exact properties which are similar to those of the propagator, \mathcal{G} , and the self-energy, Σ . We briefly recall them here in the energy representation. First, we introduce the analytical continuations, $\Pi(Z)$ and $T(Z)$, into the upper and lower complex energy half-planes, together with the associated spectral functions, $P(\Omega)$ and $\mathcal{F}(\Omega)$,

$$\Pi(Z) \equiv \int_{-\infty}^{+\infty} \frac{d\Omega}{2\pi} \frac{P(\Omega)}{Z - \Omega}, \quad (119a)$$

$$T(Z) \equiv V^{(2)} + \int_{-\infty}^{+\infty} \frac{d\Omega}{2\pi} \frac{\mathcal{F}(\Omega)}{Z - \Omega}, \quad (119b)$$

such that we recover

$$\Pi(Z = i\Omega_p) = \Pi(\Omega_p), \quad (120a)$$

$$T(Z = i\Omega_p) = T(\Omega_p). \quad (120b)$$

The T -matrix and the bubble verify the analytically extended equation

$$T(Z) = V^{(2)} + \frac{1}{2} V^{(2)} \Pi(Z) T(Z). \quad (121)$$

The corresponding retarded and advanced components are defined, as usual, by functions with arguments infinitesimally close to the real energy axis,

$$\Pi^{R/A}(\Omega) \equiv \Pi(\Omega \pm i\eta), \quad (122a)$$

$$T^{R/A}(\Omega) \equiv T(\Omega \pm i\eta). \quad (122b)$$

The corresponding spectral functions can be obtained from the discontinuities across the real axis, expressed here

as differences between advanced and retarded components,

$$P(\Omega) = i [\Pi^R(\Omega) - \Pi^A(\Omega)], \quad (123a)$$

$$\mathcal{F}(\Omega) = i [T^R(\Omega) - T^A(\Omega)]. \quad (123b)$$

Second, we enumerate the symmetry properties on the spectral functions, which translate directly on the corresponding analytical continuations. For the bubble and the T -matrix, the antisymmetry and Hermitian properties read

$$P(\Omega) = -P^T(-\Omega), \quad P(\Omega) = P^\dagger(\Omega), \quad (124a)$$

$$\mathcal{F}(\Omega) = -\mathcal{F}^T(-\Omega), \quad \mathcal{F}(\Omega) = \mathcal{F}^\dagger(\Omega). \quad (124b)$$

Regarding the positive definiteness of the spectral functions, we have¹³

$$\forall \Omega > 0, \quad P(\Omega) \succ 0, \quad \mathcal{F}(\Omega) \succ 0, \quad (126a)$$

$$P(0) = 0, \quad \mathcal{F}(0) = 0, \quad (126b)$$

$$\forall \Omega < 0, \quad P(\Omega) \prec 0, \quad \mathcal{F}(\Omega) \prec 0. \quad (126c)$$

Last, the previous expressions allow us to find the following dispersion relations for the bubble

$$\overline{\text{Re}} \Pi^{R/A}(\Omega) = \mathcal{P} \int_{-\infty}^{+\infty} \frac{d\Omega'}{2\pi} \frac{P(\Omega')}{\Omega - \Omega'}, \quad (127a)$$

$$\overline{\text{Im}} \Pi^{R/A}(\Omega) = \mp \frac{1}{2} P(\Omega), \quad (127b)$$

and for the T -matrix,

$$\overline{\text{Re}} T^{R/A}(\Omega) = V^{(2)} + \mathcal{P} \int_{-\infty}^{+\infty} \frac{d\Omega'}{2\pi} \frac{\mathcal{F}(\Omega')}{\Omega - \Omega'}, \quad (128a)$$

$$\overline{\text{Im}} T^{R/A}(\Omega) = \mp \frac{1}{2} \mathcal{F}(\Omega). \quad (128b)$$

3. Explicit solution

As mentioned earlier, a key advantage of the ladder approximation is the fact that an explicit solution for the in-medium T -matrix can be found. The Bethe-Salpeter equation for $T(Z)$ is solved in terms of the bare two-body interaction, $V^{(2)}$, and the bubble, $\Pi(Z)$, so that

$$T(Z) = V^{(2)} \left(1 - \frac{1}{2} \Pi(Z) V^{(2)} \right)^{-1}. \quad (129)$$

¹³ The positive definiteness of $\mathcal{F}(\Omega)$ is readily obtained from that of $P(\Omega)$ and the generalised optical theorem satisfied by the T -matrix [80, 81], which reads

$$\mathcal{F}(\Omega) = T^R(\Omega) P(\Omega) T^{R\dagger}(\Omega). \quad (125)$$

To have a direct connection with the propagator, we need to relate explicitly the (two-body) bubble to the (one-body) propagator. We do this in the energy representation. Fourier transforming Eq. (112c), we find

$$\Pi_{MN}(\Omega_p) = -\frac{1}{\beta} \sum_q \mathcal{G}_{\mu_1\nu_1}(\omega_q) \mathcal{G}_{\mu_2\nu_2}(\Omega_p - \omega_q), \quad (130)$$

where the multi-indices are $M = (\mu_1, \mu_2)$ and $N = (\nu_1, \nu_2)$. Therefore, plugging Eq. (130) into Eq. (129) with $Z = i\Omega_p$, we find an explicit functional of the T -matrix as a function of the propagator, $T[\mathcal{G}]$. Together with $\mathcal{G}^{\text{Dyson}}[\Sigma]$ and $\Sigma^{\text{EoM}}[\mathcal{G}, T]$, we obtain the complete set of equations for the self-consistent cycle in the ladder approximation.

For future numerical applications, we represent the expressions in terms of spectral functions only. We start by relating $\mathcal{T}(\Omega)$ to $S(\omega)$. From Eq. (129) and Eq. (123b), the spectral function of the T -matrix reads

$$\mathcal{T}(\Omega) = iV^{(2)} \left[\left(1 - \frac{1}{2} \Pi^R(\Omega) V^{(2)} \right)^{-1} - \left(1 - \frac{1}{2} \Pi^A(\Omega) V^{(2)} \right)^{-1} \right]. \quad (131)$$

Combined with the dispersion relations of the bubble given in Eqs. (127), we obtain an explicit functional $\mathcal{T}[P]$. To complete the relation between $\mathcal{T}(\Omega)$ and $S(\omega)$ we must express the spectral function of the bubble $P(\Omega)$ in terms of $S(\omega)$. The functional $P[S]$ is straightforwardly obtained from Eq. (130) which reads, in terms of spectral functions,

$$P_{MN}(\Omega) = \frac{1}{b(\Omega)} \int_{-\infty}^{+\infty} \frac{d\omega}{2\pi} S_{\mu_1\nu_1}(\omega) f(\omega) \times S_{\mu_2\nu_2}(\Omega - \omega) f(\Omega - \omega), \quad (132)$$

where $b(\Omega) \equiv \frac{1}{e^{\beta\Omega} - 1}$ is the Bose-Einstein distribution function.

Having found the relation between $\mathcal{T}(\Omega)$ and $S(\omega)$, we now need to relate $\mathcal{T}(\Omega)$ to the width $\Gamma(\omega)$ (and Σ^∞) by using $\Sigma^{\text{EoM}}[\mathcal{G}, T]$. In the particular case of the ladder approximation, the two-loop Feynman diagram of Eq. (102), shown in Fig. 5, can be simplified. Eventually, we find that

$$\Gamma_{\mu\nu}(\omega) = -\frac{1}{3} \sum_{\lambda_1\lambda_2} \int_{-\infty}^{+\infty} \frac{d\omega'}{2\pi} [f(\omega') + b(\omega' - \omega)] \times \mathcal{T}_{\mu\lambda_1\lambda_2\nu}(\omega - \omega') S^{\lambda_1\lambda_2}(\omega'). \quad (133)$$

Regarding the instantaneous part of the self-energy, Σ^∞ , we obtain it by computing the tadpole given in Eq. (102) (also shown in Fig. 5). To express it in terms of spectral functions, we use the HFB self-energy expression of Eq. (90). Since we assume only two-body interactions, the instantaneous self-energy simply reads

$$\Sigma_{\mu_1\mu_2}^\infty = \frac{1}{2} \sum_{\mu_3\mu_4} v_{[\mu_1\mu_2\mu_3\mu_4]}^{(2)} \int_{-\infty}^{+\infty} \frac{d\omega}{2\pi} f(-\omega) S^{\mu_3\mu_4}(\omega). \quad (134)$$

To close the self-consistent cycle in terms of spectral functions only, all that is left to do is to relate $S(\omega)$ with $\Gamma(\omega)$ and Σ^∞ . This has already been done in Sec. III C, with the help of Eq. (79). A step-by-step summary on the self-consistent cycle in the ladder approximation is provided later on, in Sec. IV C 5. Before this synthesis, however, we discuss the validity of the explicit solution given in Eq. (129) in terms of its convergence as a series.

4. Convergence of the series of ladders

Although the T -matrix equation can be put formally in the explicit form of Eq. (129), we must ensure that the solution is mathematically well-defined and physically meaningful. Thouless, in his pioneering work of Ref. [82], argued that the infinite series of ladder diagrams must be convergent. Put differently, the kernel of the equation must satisfy

$$\forall \Omega_p, r \left(\frac{1}{2} \Pi(\Omega_p) V^{(2)} \right) < 1, \quad (135)$$

where $r(M)$ denotes the spectral radius of the operator M , i.e.

$$r(M) \equiv \sup \{ |\lambda|, \lambda \in \sigma(M) \}, \quad (136)$$

and $\sigma(M)$ denotes the spectrum of M . In Thouless' work, the main argument for not allowing any eigenvalue to be strictly greater than 1 was that, in the case of homogeneous matter, the infinite volume limit would be ill-defined. Anticipating whether the series of ladders will be convergent or not for any general propagator is a difficult problem. Instead, we focus here on the simpler case of assuming a HFB unperturbed propagator. This case is relevant to ensure the convergence of (at least) the first iteration in the self-consistent cycle, when an HFB propagator is taken as a starting point.

In Ref. [82], Thouless studied when the condition (135) was satisfied in the context of homogeneous matter. His derivations assumed an Hermitian two-body interaction that is separable in terms of the relative incoming and outgoing momenta. Under some additional simplifying assumptions on the potential, Thouless showed that the condition (135) is equivalent to using an unperturbed propagator associated to a local minimum of the Bardeen-Cooper-Schrieffer (BCS) energy. Eventually, this leads to the well-known statement that the critical temperature of a superfluid transition, T_c , corresponds to the temperature at which the series of ladders with a normal propagator (i.e. conserving particle-number symmetry) diverges at zero energy and total momentum.

In the case of a general, Hermitian two-body interaction, we show in App. D 1 that the stability of the complex general HFB self-energy is a *necessary condition* for the series of ladders to converge at any energy. More precisely, the stability of the HFB self-energy is equivalent to the

following statement about the spectral radius of the T -matrix kernel:

$$r\left(\frac{1}{2}\Pi(0)V^{(2)}\right) < 1. \quad (137)$$

We note that, unlike Eq. (135), the kernel here is evaluated at $\Omega_p = 0$. When changing the temperature, the series of ladders at zero energy converges if and only if the HFB self-energy is stable. With this demonstration, we extend Thouless' criterion to the case of a general Hermitian two-body interaction - without any assumptions about its separability. The critical temperature T_c of a phase transition corresponds to the temperature at which the series of ladders at zero energy starts to diverge.

Although this criterion is useful to determine the critical temperature, the stability of the HFB self-energy does not appear to be sufficient to ensure the convergence of the series of ladders at *any* energy. This is crucial in our case to have a well-defined many-body approximation. This convergence problem was studied at zero temperature by Balian and Mehta [83] for a generic pairing interaction. Eventually, their proof relating the stability of the BCS energy and the convergence of the series of ladders at any energy turned out to be incomplete, due to the presence of what they refer as essential singular points [84]. This suggests that the original argument of Thouless to ensure convergence of the series of ladders at any energy relies too strongly on the simplifying assumptions made in Ref. [82].

Having said that, in practical applications such as in the study of the BCS-BEC crossover [85], the series of ladders in the normal phase are typically observed to diverge at non-zero energies *before* reaching the superfluid phase. When this happens, the divergence is interpreted as the occurrence of a pseudogap in the weak-coupling regime, or a bosonic mode in the strong-coupling regime [86–88]. Those pre-pairing effects occur between the critical temperature T_c and a temperature T_d , which we choose to define as

$$T_d \equiv \sup \left\{ T, \exists \Omega_p, r\left(\frac{1}{2}\Pi(\Omega_p)V^{(2)}\right) > 1 \right\}. \quad (138)$$

We refer to T_d as the *dynamical pairing temperature*, since it characterises a regime where the T -matrix is divergent at an energy which is not necessarily zero. In contrast, T_c is purely related to static, zero-energy effects. We note that, in the literature, many different ways of evaluating the temperature regime where pre-pairing effects occur have been proposed. For example, Ref. [89] introduces two different pseudogap temperatures and Ref. [90] defines a crossover temperature which is compared to a pair dissociation temperature. To avoid confusions, we chose a notation which departs from the usual T^* , which is typically used to denote all these analogous (yet different) temperatures.

Being able to estimate T_d in a general case, to have an idea of the regime where pre-pairing effects can play an important role, is crucial. These effects matter in

various areas of physics, such as in the study of high- T_c superconductors, of ultra-cold Fermi gases and of nuclear systems. For reviews on those systems and how their superfluid properties are connected, we refer the reader to Refs. [91, 92]. Regarding the existence of a pseudogap and its impact on observables, the question still remains open for both the unitary Fermi gas [93, 94] and infinite nuclear matter [95, 96]. In this context, we have derived a *sufficient condition* that ensures the convergence of the series of ladders at *any energy*, thus allowing to exclude dynamical pairing effects whenever such condition is satisfied. Similarly to Thouless' criterion, the condition is formulated as a strong stability condition on the HFB self-energy. To be precise, we show in App. D 2 that the series of ladders converges at any energy if

$$\left\| \frac{1}{2}\Pi(0)V^{(2)} \right\|_{\mathcal{S}_\infty} < 1, \quad (139)$$

where $\|M\|_{\mathcal{S}_\infty}$ denotes the supremum of the singular values of an operator M , i.e.

$$\|M\|_{\mathcal{S}_\infty} \equiv \sup \{ \sqrt{s}, s \in \sigma(M^\dagger M) \}. \quad (140)$$

The condition (139) is said to be strong because it implies the standard stability condition (137), thanks to the following property

$$\forall M, r(M) \leq \|M\|_{\mathcal{S}_\infty}. \quad (141)$$

More details on that condition and its derivation are given in App. D 2.

Let us consider a standard scenario, where the temperature of the physical system decreases steadily, starting from the normal phase down to the superfluid phase. Starting from the normal phase, we first hit the temperature T_s , defined as the temperature where the equality

$$\left\| \frac{1}{2}\Pi(0)V^{(2)} \right\|_{\mathcal{S}_\infty} = 1 \quad (142)$$

is satisfied. The physical system will be in a normal phase for $T > T_s$ and in a superfluid phase for $T < T_c$. Dynamical pairing effects can only occur in the regime $T_c < T < T_s$, where the conditions

$$r\left(\frac{1}{2}\Pi(0)V^{(2)}\right) < 1 < \left\| \frac{1}{2}\Pi(0)V^{(2)} \right\|_{\mathcal{S}_\infty} \quad (143)$$

are satisfied. In this scenario, Eq. (142) defines an upper-bound on T_d , i.e.

$$T_c \leq T_d \leq T_s \quad (144)$$

It is remarkable that, under some quite general assumptions, the dynamical pairing instability that generates a divergence of the series of ladders (at an energy which is not necessarily zero), can be estimated on the basis of purely static considerations at the mean-field level.

There are two interesting cases where the conditions (137) and (139) become equivalent to the convergence of the series of ladders at any energy. The first one is the limit of a weakly interacting many-body system. In this trivial case, Thouless' criterion becomes asymptotically valid, as observed in the context of ultra-cold Fermi gases [85]. A second, more interesting case, detailed in App. D3, concerns two-body interactions that are separable in the sense that there exist two (0,2)-tensors v and v' such that

$$V_{MN}^{(2)} = v_M v'_N. \quad (145)$$

This case is in close connection with the one originally studied by Thouless [82]. However, the two-body interactions considered in Ref. [82] were assumed to be separable only for relative incoming and outgoing momenta. Because of the total momentum conservation and the spin dependence, the two-body interactions were not separable in the same sense as Eq. (145), thus leaving open the possibility that $T_c < T_s$. In the sub-case where the two-body interaction is separable for relative incoming/outgoing momenta *and* non-zero only between spin singlet states of zero total momentum, the separability of Eq. (145) is recovered and Thouless' criterion holds as it was shown by an exact calculation in Ref. [97]. These considerations shed some new light on the shortcomings of Thouless' criterion regarding dynamical pairing instabilities and on the existence of pre-pairing effects in the case of strongly interacting fermions like in the BCS-BEC crossover or in nuclear systems.

In this section, considerations on the convergence of the series of ladders have been quite general. We do not discuss whether (or how) better bounds on T_d can be found in the general case. Further investigations on physical systems of interest, where the interactions are known, are also left out of the scope of this paper. In particular, if the criterion of Eq. (142) is to be useful in practice, one should check whether or not T_s remains close to T_d in typical cases of interest.

5. Summary

We recapitulate here the set of equations which are to be solved in the self-consistent ladder approximation. These are summarised succinctly for ease of access, and showcase the potential of NC-SCGF to generate formally simple expressions to describe physical systems in symmetry-broken phases.

Before doing so, we want to emphasise that the equations for the self-consistent cycle can be written down in several ways. One possible formulation of the self-consistent cycle could focus on the different objects ($\mathcal{G}, \Sigma, T, \Pi$). Working directly on these objects is problematic numerically. In particular, at zero-temperature, the self-energy undergoes drastic variations around its poles [73]. This issue stems from the presence of isolated poles for finite systems and it is worsened when

Step	Eq.	Instruction
1	(132)	$P_{MN}(\Omega) = \frac{1}{b(\Omega)} \int_{-\infty}^{+\infty} \frac{d\omega}{2\pi} S_{\mu_1\nu_1}(\omega) f(\omega) \times S_{\mu_2\nu_2}(\Omega - \omega) f(\Omega - \omega)$
2	(127a)	$\bar{\text{Re}} \Pi^{R/A}(\Omega) = \mathcal{P} \int_{-\infty}^{+\infty} \frac{d\Omega'}{2\pi} \frac{P(\Omega')}{\Omega - \Omega'}$
3	(131)	$\mathcal{T}(\Omega) = iV^{(2)} \left[\left(1 - \frac{1}{2}\Pi^R(\Omega)V^{(2)} \right)^{-1} - \left(1 - \frac{1}{2}\Pi^A(\Omega)V^{(2)} \right)^{-1} \right]$
4	(133)	$\Gamma_{\mu\nu}(\omega) = -\frac{1}{3} \sum_{\lambda_1\lambda_2} \int_{-\infty}^{+\infty} \frac{d\omega'}{2\pi} [f(\omega') + b(\omega' - \omega)] \times \mathcal{T}_{\mu\lambda_1\lambda_2\nu}(\omega - \omega') S^{\lambda_1\lambda_2}(\omega')$
5	(134)	$\Sigma_{\mu_1\mu_2}^{\infty} = \frac{1}{2} \sum_{\mu_3\mu_4} v_{[\mu_1\mu_2\mu_3\mu_4]}^{(2)} \times \int_{-\infty}^{+\infty} \frac{d\omega}{2\pi} f(-\omega) S^{\mu_3\mu_4}(\omega)$
6	(74)	$\bar{\text{Re}} \Sigma^{R/A}(\omega) = \Sigma^{\infty} + \mathcal{P} \int_{-\infty}^{+\infty} \frac{d\omega'}{2\pi} \frac{\Gamma(\omega')}{\omega - \omega'}$
7	(80)	$S(\omega) = i \left(\omega - U - \Sigma^R(\omega) \right)^{-1} - i \left(\omega - U - \Sigma^A(\omega) \right)^{-1}$

TABLE I. Equations to be solved numerically for the self-consistent ladder approximation.

working with discrete single-particle bases. In practice, this problem is circumvented by reformulating the Dyson-Schwinger and the Bethe-Salpeter equations as energy-independent eigenvalue problems [74, 98–100]. Their solutions give the spectroscopic amplitudes and pole positions of the Green's functions [24, 101]. Combining this approach to Krylov projection techniques [29, 62], SCGF calculations are routinely carried out for medium-mass nuclei [102] and reached masses of $A=138$ [103].

Alternatively, in the context of infinite nuclear matter,

SCGF calculations at non-zero temperature were carried out in the ladder approximation without symmetry-breaking [47, 48, 54, 63, 64, 104–106] in a continuous plane-wave single-particle basis. In this case, the spectral functions are continuous and the self-consistent problem is more easily handled numerically when expressed in terms of those. Note that the two numerical approaches above are complementary in the sense that one takes care of isolated poles on the real axis (associated to a discrete set of states) and the other takes care of branch cuts (associated to a continuous set of states).

For simplicity, we concentrate here on the second approach. In this case, we choose to focus on the spectral functions $(S, \Sigma^\infty, \Gamma, \mathcal{T}, P)$. The set of equations to be solved for the self-consistent ladder approximation are gathered in Table I. The corresponding iterative cycle is also pictured as a flowchart in Fig. 12 for clarity. Suppose we start the iterative cycle with a given spectral function $S^{(n)}(\omega)$. The equations displayed in Table I give back, after a full cycle, an updated spectral function $S^{(n+1)}(\omega)$. The calculation is considered to be converged when changes in the spectral function from one cycle to the next remain below a certain tolerance. At that point, we obtain the spectral functions $(S, \Sigma^\infty, \Gamma, \mathcal{T}, P)$ in the self-consistent ladder approximation. We stress that after the equations of Table I are solved self-consistently, the knowledge of the spectral functions allows us to derive the one- and two-body Green's functions in the self-consistent ladder approximation. From these, we can obtain any one- and two-body observables, including macroscopic properties, like the total energy and the thermodynamics, or microscopic data, like pairing gaps or single-particle spectra.

Finally, let us stress that all the equations of Table I have been derived in the Nambu-covariant formalism. Since all equations are expressed in terms of Nambu tensors, the equations for the self-consistent ladder approximation remain valid after any Bogoliubov transformation.

V. CONCLUSIONS

The theory of Self-Consistent Green's Function (SCGF) has been reformulated in a Nambu-covariant fashion, a substantial formal advance to treat symmetry-broken systems. We have dubbed this new formalism Nambu-covariant Self-Consistent Green's function (NC-SCGF). This step forward is achieved by expressing Green's functions and other many-body objects in terms of Nambu tensors, as introduced in Part I of our work [1]. This formalism can be applied to study many-body systems at non-zero temperatures, and can incorporate the effect of two-, three- and higher many-body interactions. While most of the exact properties have been shown to remain valid under any Bogoliubov transformation, we have also exposed examples which remain valid only up to the action of a restricted group. For example, this is the case of the GMK sum rule which, in its standard formulation,

remains valid only up to a change of single-particle bases.

In addition, taking advantage of the synthetic Nambu-covariant formalism, several exact properties have been revisited. We have shown that the positivity bound on the diagonal elements of the spectral function is a consequence of a more general definite positiveness property. From it, we have deduced additional positivity bounds for diagonal and off-diagonal elements of the spectral function.

The standard, symmetry-conserving, interpretation of the spectral function of the propagator, $S(\omega)$, is drawn from the combination of quasiparticle Lorentzian-like resonances embedded in a smooth background. In the case where the tensor $U + \Sigma^{R/A}(\omega)$ is not normal, the tensor $U + R(\omega)$ does not commute with $\Gamma(\omega)$, precluding the previous interpretation. This led us to introduce the line-shape tensor, $\Theta(\omega)$, which can be interpreted physically as a characterisation of interferences between the damped propagation of a quasiparticle state in the residual medium and the excitation of a continuum of modes displayed by the residual medium. The quasiparticle resonances in the spectrum of $S(\omega)$ become Fano-like resonances, and their line shapes are related to $\Theta(\omega)$. Eventually, we have argued that $\Theta(\omega)$ provides an interesting indicator of the combined importance of correlations and symmetry-breaking within a many-body system.

Building on the NC-SCGF formalism, we can formulate Nambu-covariant approximations that are self-consistent not only in the propagator, but also in the two-body vertex. We have paid specific attention to the self-consistent ladder approximation by giving it an explicit formulation, valid for symmetry-broken phases and for a general two-body interaction. The self-consistent cycle boils down to seven equations, shown in Table I, for the spectral functions of the propagator, the self-energy, the in-medium T -matrix and the bubble propagator. Thanks to the Nambu-covariant formalism introduced in Part I, these equations display a formal complexity which is similar to those in the symmetry-conserving case. This is a crucial step towards an efficient numerical implementation of the self-consistent ladder approximation in symmetry-breaking phases. Applications to superfluid nuclear matter will be reported in a future work.

Along these lines, we have also revisited the question of the convergence of the series of ladders for a complex general HFB propagator. We have shown that Thouless' criterion, commonly used to determine the critical temperature T_c , remains valid in the case of a complex general HFB propagator and a general Hermitian two-body interaction. We have also proposed a new criterion to determine a pre-pairing temperature, T_s , such that dynamical pairing instabilities generating singularities in the (non self-consistent) T -matrix can only occur at temperatures $T_c < T < T_s$.

Finally, let us mention two immediate developments that could stem from this work. First, to go beyond the self-consistent ladder approximation, one can consider corrections to the irreducible part of the Bethe-Salpeter equation. For example, this has been done in the

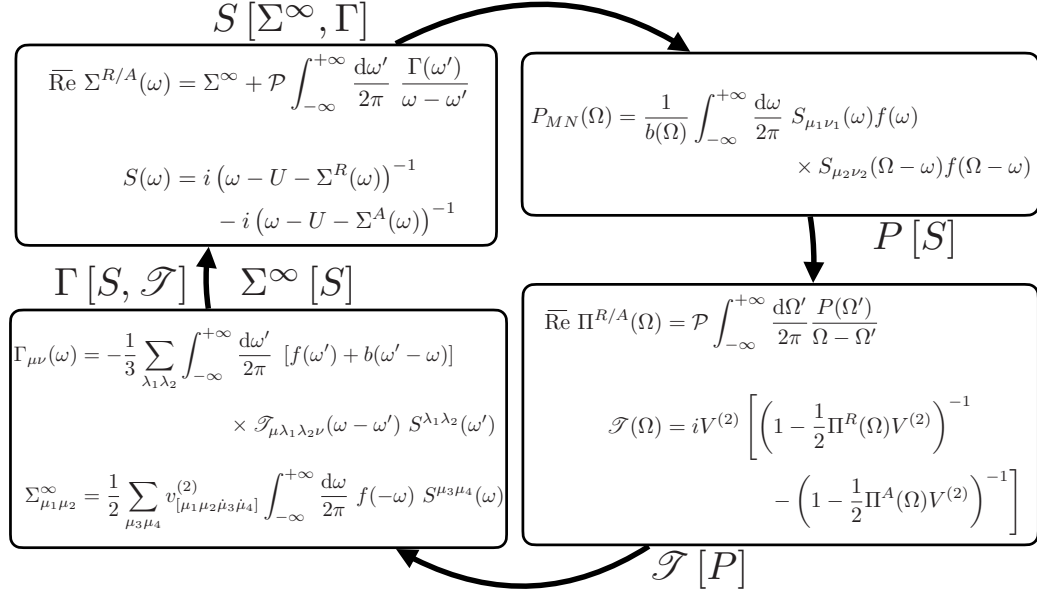


FIG. 12. Flowchart representing the self-consistent cycle obtained by iterating the self-consistent ladder approximation expressed in terms of $(S, \Sigma^\infty, \Gamma, \mathcal{T}, P)$. Equations displayed in the flowchart corresponds to those gathered in Table. I.

symmetry-conserving case at zero temperature for application to atomic nuclei [74]. Alternatively, the T -matrix can be used as an effective interaction vertex in the spirit of the Brueckner-Bethe-Goldstone method (see Ref. [107] for an introductory review). Second, beyond purely diagrammatic considerations, the formalism of NC-SCGF opens up new avenues towards the restoration of symmetries. While many-body approximations such as CC and MBPT have been extended to include breaking and restoration of symmetries [3, 108], no restoration procedure has been designed and implemented for SCGF approximations, despite its critical role in applications to finite systems such as atomic nuclei [8, 109, 110]. In Refs. [3, 108], the restoration of symmetries was designed at zero temperature by mixing several single-reference calculations with vacua related by non-unitary Bogoliubov transformations. Studying the problem of symmetry-restoration in terms of Nambu tensors, which, by design, are covariant with respect to non-unitary Bogoliubov transformations, could shed new light on the restoration of symmetries within SCGF schemes.

ACKNOWLEDGMENTS

The authors thank J. W. T. Keeble for proofreading the manuscript. M. D. would like to thank T. Duguet for pointing him to the work of R. Balian and M. L. Mehta on the convergence of the series of ladders at zero temperature [83, 84].

This work is supported by STFC, through Grants Nos ST/L005743/1 and ST/P005314/1; by the Span-

ish MICINN through the “Ramón y Cajal” program with grant RYC2018-026072 and the “Unit of Excellence María de Maeztu 2020-2023” award to the Institute of Cosmos Sciences (CEX2019-000918-M).

Appendix A: Hermitian conjugate tensor

In this appendix, we give a precise definition of the Hermitian conjugate of a tensor. First we focus on $(1, 1)$ -tensors where the definition is identical to the adjoint of an operator with respect to a given Hermitian product. Then, we extend the concept of Hermitian conjugation to (p, q) -tensors where $p + q = 2k$ and k is a natural number.

1. Hermitian conjugation for $(1,1)$ -tensors

Let $h(\cdot, \cdot)$ be the Hermitian product defined on \mathcal{H}_1^e by

$$h\left(\begin{pmatrix} |\Psi_1\rangle \\ \langle\Psi'_1| \end{pmatrix}, \begin{pmatrix} |\Psi_2\rangle \\ \langle\Psi'_2| \end{pmatrix}\right) \equiv \langle\Psi_1 | \Psi_2\rangle + \langle\Psi'_2 | \Psi'_1\rangle. \quad (\text{A1})$$

Let us stress that $h(\cdot, \cdot)$ is related to, but different, from $g(\cdot, \cdot)$ defined in Part I. We use this Hermitian product to define the notion of orthogonality of an extended basis, i.e. a basis $\mathcal{B}^e = \{|\mu'\rangle\}$ is orthogonal if and only if

$$h(|\mu'\rangle, |\nu'\rangle) = \delta_{\mu'\nu'}. \quad (\text{A2})$$

We also use this Hermitian product to define the Hermitian conjugate of a linear operator t , acting on \mathcal{H}_1^e , as

the unique linear operator t^\dagger verifying

$$h \left(\begin{pmatrix} |\Psi_1\rangle \\ \langle \Psi'_1| \end{pmatrix}, t \begin{pmatrix} |\Psi_2\rangle \\ \langle \Psi'_2| \end{pmatrix} \right) \equiv h \left(t^\dagger \begin{pmatrix} |\Psi_1\rangle \\ \langle \Psi'_1| \end{pmatrix}, \begin{pmatrix} |\Psi_2\rangle \\ \langle \Psi'_2| \end{pmatrix} \right). \quad (\text{A3})$$

Eventually, the Hermitian conjugation is transported to $(1, 1)$ -tensors by using the canonical identification of $(1, 1)$ -tensors to linear operators. In practice, t^\dagger is the unique $(1, 1)$ -tensor whose coordinates verify

$$(t^\dagger)^\mu{}_\nu = (t^\nu{}_\mu)^* \quad (\text{A4})$$

in any *orthogonal* basis $\mathcal{B}^{e'}$.

If $\mathcal{B}^{e'}$ is not orthogonal, the relation in Eq. (A4) no longer holds. Conversely, if, in an orthogonal basis, two $(1, 1)$ -tensors r and s verify

$$r^\mu{}_\nu = (s^\nu{}_\mu)^*, \quad (\text{A5})$$

then they verify

$$r^\mu{}_\nu = (s^\dagger)^\mu{}_\nu \quad (\text{A6})$$

in *any* basis. We say that r is the Hermitian conjugate tensor of s .

This notion of Hermitian conjugation allows us to introduce the unitary group $U(\mathcal{H}_1^e)$ defined as the sub-group of $GL(\mathcal{H}_1^e)$ characterised by a transformation $\mathcal{W}^\mu{}_\nu$ verifying

$$\sum_\lambda \mathcal{W}^\mu{}_\lambda (\mathcal{W}^\dagger)^\lambda{}_\nu = g^\mu{}_\nu = \delta_{\mu\nu}. \quad (\text{A7})$$

Note that $GL(\mathcal{H}_1^e)$ contains the sub-group $O(\mathcal{H}_1^e, g)$ which is a faithful representation of Bogoliubov transformations, while $U(\mathcal{H}_1^e)$ only contains the sub-group $O(\mathcal{H}_1^e, g) \cap U(\mathcal{H}_1^e)$ which is a faithful representation of *unitary* Bogoliubov transformations.

In this paper, we make use extensively of the Hermitian conjugation of tensors. This allows us to write equations which are invariant under Bogoliubov transformations, rather than invariant under unitary Bogoliubov transformations only. To see this, compare for example Eq. (A5) and Eq. (A6) whose groups of invariance are, respectively, $U(\mathcal{H}_1^e)$ and $GL(\mathcal{H}_1^e)$. In addition, in this paper our working basis \mathcal{B}^e is orthogonal, so whenever we derive an equation like Eq. (A5) in \mathcal{B}^e , we can and will straightforwardly generalise it to an equation of the type of Eq. (A6).

2. Extensions

So far we have only defined the Hermitian conjugate of a $(1, 1)$ -tensor. To generalise this definition to (p, q) -tensors with $p + q = 2k$, we first focus on (k, k) -tensors. We will subsequently extend the definition by compatibility with the raising and lowering of indices with the metric g .

a. (k, k) -tensors

Tensors of type (k, k) are canonically associated with linear operators acting on $\mathcal{H}_1^{e \otimes k}$. To define the Hermitian conjugate of a linear operator t acting on $\mathcal{H}_1^{e \otimes k}$, we use the Hermitian product defined by

$$h^{(k)}(u_1 \otimes \dots \otimes u_k, v_1 \otimes \dots \otimes v_k) \equiv \prod_{i=1}^k h(u_i, v_i), \quad (\text{A8})$$

where u_i and v_i are vectors of \mathcal{H}_1^e . We associate a unique linear operator t^\dagger to a linear operator t acting on $\mathcal{H}_1^{e \otimes k}$, verifying

$$\begin{aligned} h^{(k)}(u_1 \otimes \dots \otimes u_k, t(v_1 \otimes \dots \otimes v_k)) \\ \equiv h^{(k)}(t^\dagger(u_1 \otimes \dots \otimes u_k), v_1 \otimes \dots \otimes v_k). \end{aligned} \quad (\text{A9})$$

The Hermitian conjugation of (k, k) -tensors is then defined by canonical identification of (k, k) -tensors with linear operators acting on $\mathcal{H}_1^{e \otimes k}$. In practice, for any (k, k) -tensor t , its Hermitian conjugate is the unique (k, k) -tensor t^\dagger whose coordinates verify in any *orthogonal* basis

$$(t^\dagger)^M{}_N = (t^N{}_M)^*. \quad (\text{A10})$$

For convenience we have used the k -dimensional multi-indices

$$M \equiv (\mu_1, \dots, \mu_k), \quad (\text{A11a})$$

$$N \equiv (\nu_1, \dots, \nu_k), \quad (\text{A11b})$$

so that tensor coordinates of a (k, k) -tensor are denoted as

$$t^M{}_N \equiv t^{\mu_1 \dots \mu_k}{}_{\nu_1 \dots \nu_k}. \quad (\text{A12})$$

In particular, let us stress that the k^{th} tensor power of our working basis $\mathcal{B}^{e \otimes k}$ is orthogonal with respect to $h^{(k)}(\cdot, \cdot)$. Note also that this definition of the Hermitian conjugation is compatible with the previous one for $(1, 1)$ -tensors.

b. Metric compatibility

We define the Hermitian conjugate of a (p, q) -tensor with $p + q = 2k$ and k a natural number, by compatibility with the raising and lowering of indices with the metric g . In our working basis \mathcal{B}^e , which is orthogonal with respect to $h(\cdot, \cdot)$, the metric verifies

$$g^{\mu\nu} = (g_{\nu\mu})^*. \quad (\text{A13})$$

Consequently, we can define the Hermitian conjugate of a $(0, 2k)$ -tensor as the unique $(2k, 0)$ -tensor whose coordinates verify

$$(t^\dagger)^{MN} = (t_{NM})^*, \quad (\text{A14})$$

in any orthogonal basis. Similar definitions hold for all the associated type (p, q) of tensors with $p + q = 2k$.

A (p, q) -tensor t (with $p + q = 2k$) is said to be Hermitian or anti-Hermitian, respectively, when¹⁴

$$t^\dagger = t, \quad (\text{A15a})$$

$$t^\dagger = -t. \quad (\text{A15b})$$

For example, since \mathcal{B}^e is orthogonal and the metric satisfies Eq. (A13), we have

$$g = g^\dagger \quad (\text{A16})$$

i.e. the metric is Hermitian. Finally, a (p, q) -tensor t with $p + q = 2k$ will be said to be unitary if and only if

$$t^\dagger t = t t^\dagger = g, \quad (\text{A17})$$

where the product of tensors is defined in App. B.

Appendix B: Functional calculus

In this appendix, we specify the functional calculus that is used in this paper and that is necessary to develop the NC-SCGF formalism. In other words, we provide a definition for functions depending on tensors. We follow the same approach as the previous Appendix and focus first on defining functions on $(1, 1)$ -tensors. Then, the definition is extended to (p, q) -tensors where $p + q = 2k$ and k is a natural number.

1. Functional calculus for $(1, 1)$ -tensors

Let $t^\mu{}_\nu$ be a $(1, 1)$ -tensor and $T^{1,1}(\mathcal{H}_1^e)$ be the vector space of $(1, 1)$ -tensors. We define functions on the space of $(1, 1)$ tensors in the same way as it is usually done for operators or matrices. A formal power series on $(1, 1)$ -tensors is defined such that $\forall i \in \mathbb{N}^*$,

$$(t^i)^\mu{}_\nu \equiv \sum_{\alpha_1 \dots \alpha_{i-1}} t^\mu{}_{\alpha_1} t^{\alpha_1}{}_{\alpha_2} \dots t^{\alpha_{i-2}}{}_{\alpha_{i-1}} t^{\alpha_{i-1}}{}_\nu. \quad (\text{B1a})$$

For $i = 0$, we define

$$(t^0)^\mu{}_\nu \equiv g^\mu{}_\nu = \delta_{\mu\nu}. \quad (\text{B1b})$$

Moreover, for any formal power series g_1 and g_2 and for $\lambda \in \mathbb{C}$, we define

$$(\lambda g_1 + g_2)(t) \equiv \lambda g_1(t) + g_2(t). \quad (\text{B1c})$$

Let $f(X)$ be the formal power series

$$f(X) \equiv \sum_{i=0}^{+\infty} c_i X^i, \quad (\text{B2})$$

with $c_i \in \mathbb{C}$. With the above definitions, the function f on $(1, 1)$ -tensors reads

$$f : T^{1,1}(\mathcal{H}_1^e) \rightarrow T^{1,1}(\mathcal{H}_1^e) \\ t \mapsto f(t) = \sum_{i=0}^{+\infty} c_i t^i. \quad (\text{B3})$$

Writing down the coordinates explicitly, one finds

$$f(t)^\mu{}_\nu = \sum_{i=0}^{+\infty} c_i (t^i)^\mu{}_\nu. \quad (\text{B4})$$

Note that, throughout this paper, we use the shorthand notation $t^0 = 1$.

We extend the functional calculus on $(1, 1)$ -tensors to holomorphic functions by using Cauchy's integral formula, in analogy to the case of operators and matrices. Briefly, we recall that this amounts to define

$$f(t) \equiv \frac{1}{2\pi i} \int_C f(\lambda) (\lambda - t)^{-1} d\lambda \quad (\text{B5})$$

for any function f which is holomorphic in a open set, including the spectrum of t , and for C a contour enclosing it. For more details on holomorphic calculus we refer to classical textbooks such as Ref. [111].

2. Extensions

We extend the functional calculus on $(1, 1)$ -tensors to $(0, 2)$ - and $(2, 0)$ -tensors as follows. Let $t_{\mu\nu}$ be a $(0, 2)$ -tensor. Powers $(t^i)_{\mu\nu}$ are defined such that they are compatible with raising and lowering indices starting from the definitions given in Eqs. (B1a) and (B1b). To be concrete, we have $\forall i \in \mathbb{N}^*$

$$(t^i)_{\mu\nu} \equiv \sum_{\alpha_1 \dots \alpha_{i-1}} t_{\mu\alpha_1} t^{\alpha_1}{}_{\alpha_2} \dots t^{\alpha_{i-2}}{}_{\alpha_{i-1}} t^{\alpha_{i-1}}{}_\nu, \quad (\text{B6a})$$

and, for $i = 0$,

$$(t^0)_{\mu\nu} \equiv g_{\mu\nu}. \quad (\text{B6b})$$

In analogy to $(1, 1)$ -tensors, these definitions are extended to any formal power series by linearity. The extension to holomorphic functions is performed, again, using Cauchy's integral formula. Functions of $(2, 0)$ -tensors are defined analogously to functions of $(0, 2)$ -tensors.

Finally, we extend the functional calculus to tensors of type (p, q) where $p + q = 2k$ for a natural number k . As we just did for $(0, 2)$ - and $(2, 0)$ -tensors, we only need to define functions on (k, k) -tensors. Functions on a

¹⁴ We employ a slight abuse of notation here. In principle t^\dagger is a (q, p) -tensor which is not of the same type as t . Here t^\dagger is to be understood as the (p, q) -tensor obtained after the appropriate raising and lowering operation with the metric, so that it is of the same type as t .

(p, q) -tensor are then obtained by enforcing compatibility with the raising and lowering operation of indices. Let $t^{\mu_1 \dots \mu_k}_{\nu_1 \dots \nu_k}$ be a (k, k) -tensor. For convenience, we use the same k -dimensional multi-indices

$$M \equiv (\mu_1, \dots, \mu_k), \quad (\text{B7a})$$

$$N \equiv (\nu_1, \dots, \nu_k), \quad (\text{B7b})$$

as in App. A. Powers of a (k, k) -tensor are defined such that, $\forall i \in \mathbb{N}^*$

$$(t^i)^M_N \equiv \sum_{L_1 \dots L_{i-1}} t^M_{L_1} t^{L_1}_{L_2} \dots t^{L_{i-2}}_{L_{i-1}} t^{L_{i-1}}_N, \quad (\text{B8a})$$

where L_p are dummy k -dimensional multi-indices. Again, for $i = 0$, we define

$$(t^0)^M_N \equiv \prod_{p=1}^k g^{\mu_p}_{\nu_p} = \delta_{MN}. \quad (\text{B8b})$$

Similarly to $(1, 1)$ -tensors, those definitions are extended to formal power series by linearity and to holomorphic functions using Cauchy's integral formula.

Appendix C: Interpretation of $\Theta(\omega)$

In Sec. III C 2, we introduce a tensor, $\Theta(\omega)$, which allows us to relate the self-energy to the spectral function of the propagator. In this section, we motivate the physical interpretation of $\Theta(\omega)$ as a tensor characterising the interferences between the damped propagation of quasiparticle states and the excitation of a continuum of non-resonant modes displayed by the residual medium. To justify this interpretation, we look at the impact of

$$S_{\text{pk}}(\omega) \equiv \left[\Gamma(\omega_{\text{qp}}) + 2(\omega - U - R(\omega_{\text{qp}}))\Theta(\omega_{\text{qp}}) \right] \left[\left((\omega - U - R(\omega_{\text{qp}}))^2 + \left(\frac{\Gamma(\omega_{\text{qp}})}{2} \right)^2 \right) \left(1 + \Theta^2(\omega_{\text{qp}}) \right) \right]^{-1}. \quad (\text{C3})$$

When $\Theta(\omega_{\text{qp}}) = 0$, we recover the well-known Lorentzian shape of the spectral function. We thus interpret $\Gamma(\omega_{\text{qp}})$ as a tensor generalisation of the width of a quasiparticle resonance, whose inverse is related to the life-time and mean-free path of a quasiparticle state propagating at energy ω_{qp} [65]. In other words, $\Gamma(\omega_{\text{qp}})$ characterises the damping of a quasiparticle state propagating at energy ω_{qp} in the medium.

In contrast, when $\Theta(\omega_{\text{qp}}) \neq 0$, Eq. (C3) is no longer a simple Lorentzian, but resembles instead a *Fano function* (or a Fano line-shape profile) [66]. We recall that a normalised Fano resonance, $F_q(\omega)$, is expressed in terms of the position of the resonance, ω_{qp} ; its width, Γ_{qp} ; and its

$\Theta(\omega) \neq 0$ in two approximations that are often considered in the symmetry-conserving case. We first discuss the *peak approximation*, which is obtained assuming that all the self-energy components are constant around a given quasiparticle peak energy. We then turn our attention to the *quasiparticle approximation*, which incorporates additional dispersive corrections associated to the energy dependence of Σ around the peak. These two cases turn out to provide a concordant physical picture for $\Theta(\omega)$.

1. Peak approximation

The peak approximation of the spectral function $S(\omega)$ can be interpreted as a degraded version of the standard quasiparticle approximation [65]. In this approximation, we focus on describing the spectral function around one peak, centred at an energy ω_{qp} , which is associated to a quasiparticle state. A crude way of locating these peaks consists in fixing their locus as the solutions of

$$\det[\omega_{\text{qp}} - U - R(\omega_{\text{qp}})] = 0. \quad (\text{C1})$$

The quasiparticle states are then the eigenvectors of $U + R(\omega_{\text{qp}})$ associated to the eigenvalues ω_{qp} . For energies $\omega \simeq \omega_{\text{qp}}$, the spectral function can be approximated by assuming that all the energy-dependent components of the self-energy are roughly constant and independent of the energy,

$$R(\omega) \simeq R(\omega_{\text{qp}}), \quad (\text{C2a})$$

$$\Gamma(\omega) \simeq \Gamma(\omega_{\text{qp}}), \quad (\text{C2b})$$

$$\Theta(\omega) \simeq \Theta(\omega_{\text{qp}}). \quad (\text{C2c})$$

This approximation, albeit crude, is already sufficient to motivate a physical interpretation of $\Gamma(\omega_{\text{qp}})$ in the symmetry-conserving case. The spectral function in this peak approximation reads

line-shape parameter, q , as

$$F_q(\omega) = \frac{\left(\frac{\Gamma_{\text{qp}}}{2} \right)^2 + 2 \left(\frac{\Gamma_{\text{qp}}}{2} \right) (\omega - \omega_{\text{qp}}) q^{-1} + \left(\frac{\omega - \omega_{\text{qp}}}{q} \right)^2}{\left((\omega - \omega_{\text{qp}})^2 + \left(\frac{\Gamma_{\text{qp}}}{2} \right)^2 \right) \left(1 + q^{-2} \right)}. \quad (\text{C4})$$

For an introduction and an historical perspective on Fano functions, we refer the reader to Refs. [112, 113]. The family of Fano functions, indexed over the line-shape parameter q , can be seen as an extension of a Lorentzian function. The latter is recovered in the limit $q \rightarrow +\infty$.

At finite q , the constant term in the numerator is

related to the quasiparticle resonance; the quadratic term, to the non-resonant background; and the linear term, to quasiparticle-background interferences [112]. For $|\omega - \omega_{\text{qp}}| \ll q$ we can drop the quadratic term in the numerator and we recover in essence Eq. (C3), i.e. a Lorentzian whose numerator is shifted by a linear contribution in $\omega - \omega_{\text{qp}}$. Another way to show the similarity between Eq. (C3) and a Fano function consists in rewriting Fano functions as

$$F_q(\omega) = \frac{1}{4} \frac{(\Gamma_{\text{qp}} + 2(\omega - \omega_{\text{qp}})q^{-1})^2}{\left((\omega - \omega_{\text{qp}})^2 + \left(\frac{\Gamma_{\text{qp}}}{2}\right)^2\right) \left(1 + q^{-2}\right)}. \quad (\text{C5})$$

This formula suggests a direct analogy between the line-shape parameter, q , and the inverse of the line-shape tensor, $\Theta^{-1}(\omega_{\text{qp}})$. Note, however, the difference between the numerator in Eq. (C3), which is squared, and that of Eq. (C5), which is not. A similar difference already appears in the symmetry-conserving case, where the numerator in the Lorentzian spectral function typically involves a linear (rather than quadratic) width.

In physical applications, the Fano line-shape parameter q is interpreted as the consequence of interferences between a discrete state and a competing continuum of states around the same energy ω_{qp} [112]. In the time domain, the interferences are related to a phase shift, $-2 \arctan(q^{-1})$, and a relative scaling factor, $q^2 + 1$, between the quasiparticle and the background contributions [114]. This motivates an interpretation of $\Theta(\omega_{\text{qp}})$ as a tensor characterising the interferences between the propagation of a quasiparticle state of energy ω_{qp} in the medium, and the excitation of a continuum of modes that the background displays around the energy ω_{qp} .

Despite their usefulness, these interpretations of $\Gamma(\omega_{\text{qp}})$ and $\Theta(\omega_{\text{qp}})$ are only valid for the crude peak approximation employed here. If this approximation is refined, the direct connection between $\Gamma(\omega_{\text{qp}})$ and the width of a quasiparticle resonance becomes more tenuous. The same is true for the association between $\Theta(\omega_{\text{qp}})$ and the line-shape parameter of the resonance. Moreover, it may be possible that the relation between $S_{\text{pk}}(\omega)$ and Fano functions is merely symbolic. To discard the last possibility, we now turn to the more realistic quasiparticle approximation of the spectral function and show that the spectrum of the approximated spectral function, $S_{\text{qp}}(\omega)$, displays Fano-like resonances.

2. Quasiparticle approximation and Fano spectrum

In the symmetry-conserving case, one can prove that the spectral function remains Lorentzian even when some dispersion corrections, which incorporate energy-dependent effects, are included in the description of the self-energy [49, 65]. Similarly, we now proceed to show that the shape of the resonances displayed by the spectrum of the spectral function is, in the quasiparticle approximation, closely related to a Fano resonance.

The quasiparticle approximation we consider consists in assuming that the analytic propagator, $\mathcal{G}(z)$, contains only simple isolated poles in non-physical Riemann sheets¹⁵. From Eq. (56), the locus z_{qp} of poles in the complex energy plane arise from the solutions of

$$\det[z_{\text{qp}} - U - \Sigma(z_{\text{qp}})] = 0. \quad (\text{C6})$$

Combining the Mittag-Leffler's theorem¹⁶, the asymptotic property of the analytic propagator given in Eq. (34), and the assumption of simple poles, the exact propagator can be decomposed in partial fractions and reads, for $\text{Im } z > 0$,

$$\mathcal{G}(z) = \sum_{\substack{z_{\text{qp}} \\ \text{Im } z_{\text{qp}} < 0}} \frac{G_{\text{qp}}}{z - z_{\text{qp}}} \quad (\text{C7})$$

where G_{qp} are the residues associated to the poles z_{qp} , which verify

$$G_{\text{qp}} = \frac{1}{2\pi i} \int_{C_{\text{qp}}} (z - (U + \Sigma(z)))^{-1} dz, \quad (\text{C8})$$

where C_{qp} is a positively-oriented, arbitrarily small closed path around z_{qp} . We stress that in Eq. (C7) the sum runs over poles with negative imaginary parts, $\text{Im } z_{\text{qp}} < 0$, and the equality is only valid in the positive half-plane, $\text{Im } z > 0$. The extension of Eq. (C7) to $\text{Im } z \leq 0$ would give the propagator in a non-physical Riemann sheet.

We can combine Eqs. (C7), (23) and (26a), to find the quasiparticle spectral function

$$S_{\text{qp}}(\omega) = \sum_{\substack{z_{\text{qp}} \\ \text{Im } z_{\text{qp}} < 0}} \frac{\overline{\text{Re}}(G_{\text{qp}}) \Gamma_{\text{qp}} - 2 \overline{\text{Im}}(G_{\text{qp}}) (\omega - \omega_{\text{qp}})}{(\omega - \omega_{\text{qp}})^2 + \left(\frac{\Gamma_{\text{qp}}}{2}\right)^2}, \quad (\text{C9})$$

where ω_{qp} and $-\frac{\Gamma_{\text{qp}}}{2}$ are the real and imaginary parts of z_{qp} , i.e.

$$z_{\text{qp}} \equiv \omega_{\text{qp}} - i \frac{\Gamma_{\text{qp}}}{2}. \quad (\text{C10})$$

To have a more direct relation between the residues and the self-energy, we make the additional approximation that

$$\forall z \in C_{\text{qp}}, \quad \Sigma(z) \simeq \Sigma(z_{\text{qp}}) + (z - z_{\text{qp}}) \frac{\partial \Sigma}{\partial z}(z_{\text{qp}}). \quad (\text{C11})$$

In other words, we expect that the (complex) energy dependence of the self-energy around the pole is smooth and can be accurately captured by a first-order Taylor

¹⁵ Non-physical Riemann sheets are obtained by analytically continuing the propagator through the real axis cut [65]. For technical details, we refer to the review of Ref. [115].

¹⁶ See for example pp. 299-301 of Ref. [116].

expansion. With a bit of algebra, and using the Laurent expansion of a resolvent¹⁷ around z_{qp} , we obtain

$$G_{\text{qp}} \simeq \mathcal{Z}_{\text{qp}} P_{\text{qp}} , \quad (\text{C12})$$

where P_{qp} is the eigenprojection of $U + \Sigma(z_{\text{qp}})$ associated to z_{qp} ¹⁸ and

$$\mathcal{Z}_{\text{qp}} = \frac{1}{1 - \text{Tr}_{\mathcal{H}_1^e} \left[P_{\text{qp}} \frac{\partial \Sigma}{\partial z}(z_{\text{qp}}) \right]} , \quad (\text{C13})$$

where $\text{Tr}_{\mathcal{H}_1^e}$ denotes the trace over \mathcal{H}_1^e . Since $U + \Sigma(z_{\text{qp}})$ is not necessarily Hermitian, neither is the projector P_{qp} and \mathcal{Z}_{qp} is a complex number. In the symmetry-conserving case, \mathcal{Z}_{qp} is usually referred to as the *renormalisation factor* of the quasiparticle resonance. Using Eq. (C9), the quasiparticle spectral function reads

$$S_{\text{qp}}(\omega) = \sum_{\substack{z_{\text{qp}} \\ \text{Im } z_{\text{qp}} \leq 0}} \frac{\overline{\text{Re}}(\mathcal{Z}_{\text{qp}} P_{\text{qp}}) \Gamma_{\text{qp}} - 2 \overline{\text{Im}}(\mathcal{Z}_{\text{qp}} P_{\text{qp}}) (\omega - \omega_{\text{qp}})}{(\omega - \omega_{\text{qp}})^2 + \left(\frac{\Gamma_{\text{qp}}}{2}\right)^2} . \quad (\text{C14})$$

To make the Fano resonant structure more clear, we assume the projectors to be orthogonal, so that

$$P_{\text{qp}}^\dagger = P_{\text{qp}} \quad (\text{C15})$$

and, eventually, we obtain

$$S_{\text{qp}}(\omega) = \sum_{\substack{z_{\text{qp}} \\ \text{Im } z_{\text{qp}} \leq 0}} \text{Re}(\mathcal{Z}_{\text{qp}}) \frac{\Gamma_{\text{qp}} - 2 \frac{\text{Im}(\mathcal{Z}_{\text{qp}})}{\text{Re}(\mathcal{Z}_{\text{qp}})} (\omega - \omega_{\text{qp}})}{(\omega - \omega_{\text{qp}})^2 + \left(\frac{\Gamma_{\text{qp}}}{2}\right)^2} P_{\text{qp}} . \quad (\text{C16})$$

Comparing Eq. (C16) to Eq. (C5), we clearly see that the spectrum of $S_{\text{qp}}(\omega)$ is made of resonances with line-shapes that are similar to Fano functions. These resonances occur at energies around ω_{qp} ; have a width Γ_{qp} ; a fragmentation, $\text{Re}(\mathcal{Z}_{\text{qp}})$; and a line-shape factor q_{qp} defined as

$$q_{\text{qp}} \equiv - \frac{\text{Re}(\mathcal{Z}_{\text{qp}})}{\text{Im}(\mathcal{Z}_{\text{qp}})} . \quad (\text{C17})$$

The quasiparticle state associated to a resonance is non-degenerate, and corresponds to the eigenstate of $U + \Sigma(z_{\text{qp}})$ associated to the eigenvalue z_{qp} . Interestingly, the additional assumptions made in Eqs. (C11) and (C15) imply that the analytic continuation of the line-shape tensor verifies $\Theta(z_{\text{qp}}) = 0$. However, we still

have, in general, $\Theta(\omega_{\text{qp}}) \neq 0$, which is reflected on the non-Lorentzian line-shape of the resonance at ω_{qp} .

The above analysis in the quasiparticle approximation further supports our interpretation of the tensor $\Theta(\omega)$ as a characterisation of the interferences between the propagation of a state in the medium and the excitation of a continuum of non-resonant modes displayed by the medium. In the peak approximation, the inverse of $\Theta(\omega_{\text{qp}})$ was directly proportional to a tensor generalisation of the line-shape parameter q . Here, in the quasiparticle approximation, we gain further insight by showing how the spectrum of the spectral function does display Fano-like resonances when we assume Eqs. (C11) and (C15) to hold. Future numerical implementations of the NC-SCGF approach will be able to discern the importance of Fano structures in the spectral function of many-body systems.

Appendix D: Convergence of the series of ladders

In this section, we study the convergence of the series of ladders. We assume an Hermitian two-body interaction and a complex general HFB propagator. First, we derive a straightforward extension of Thouless' criterion [82]. We show that, in general, the stability of the HFB self-energy is equivalent to the convergence of the series of ladders at zero energy. Second, we work a sufficient condition for the series to converge at *any* energy. Finally, we identify separable interactions as a special case, where the extension of Thouless' criterion is simultaneously necessary and sufficient.

1. Necessary condition

Let us show that the stability of the HFB self-energy, Σ^{HFB} , is a necessary condition for the convergence of the series of ladders with an HFB propagator. First, we recall that the HFB self-energy Σ^{HFB} is an implicit solution of Eq. (91). Since we are restricting ourselves to the case of a two-body interaction, this is equivalent to saying that the HFB self-energy is a fixed point of the functional \mathcal{F} defined by

$$\mathcal{F}[\Sigma]_{\mu\nu} = -\frac{1}{2} \sum_{\lambda_2 \lambda_3} v_{[\mu \lambda_2 \lambda_3 \nu]}^{(2)} \frac{1}{\beta} \sum_{\omega_l} \mathcal{G}[\Sigma]^{\lambda_2 \lambda_3}(\omega_l) e^{-i\omega_l \eta} , \quad (\text{D1})$$

where we recall that

$$\mathcal{G}[\Sigma](\omega_l) = (i\omega_l - (U + \Sigma(\omega_l)))^{-1} . \quad (\text{D2})$$

Physically speaking, the stability of the HFB self-energy, as a fixed point of \mathcal{F} , is important to ensure that the associated HFB state of the many-body system will not decay after an infinitesimally small external (one-body) perturbation.

To study the linear stability of the fixed point, Σ^{HFB} , of \mathcal{F} , we compute the effect of a small deviation $\delta\Sigma$ from it.

¹⁷ See for example Eq. (6.32) of Ref. [117]

¹⁸ Since the eigenspace is non-degenerate, the eigenprojection P_{qp} is simply the outer product of the unique right and left eigenvector of $U + \Sigma(z_{\text{qp}})$ associated to the eigenvalue z_{qp} .

Since \mathcal{F} gives a self-energy which is both antisymmetric and energy independent, we restrict our linear stability analysis to perturbations $\delta\Sigma$ with the same properties. From the differential of the inverse, we find the relation between $\delta\mathcal{G}$ and $\delta\Sigma$,

$$\begin{aligned} \delta\mathcal{G}[\Sigma^{\text{HFB}}](\omega_l) &\equiv \mathcal{G}[\Sigma^{\text{HFB}} + \delta\Sigma](\omega_l) - \mathcal{G}[\Sigma^{\text{HFB}}](\omega_l) \\ &= -\mathcal{G}[\Sigma^{\text{HFB}}](\omega_l) \delta\Sigma \mathcal{G}[\Sigma^{\text{HFB}}](\omega_l) . \end{aligned} \quad (\text{D3})$$

The differential of \mathcal{F} at Σ^{HFB} reads explicitly

$$\begin{aligned} \delta\mathcal{F}[\Sigma^{\text{HFB}}]_{\mu\nu} &\equiv \mathcal{F}[\Sigma^{\text{HFB}} + \delta\Sigma]_{\mu\nu} - \mathcal{F}[\Sigma^{\text{HFB}}]_{\mu\nu} \\ &= \frac{1}{2\beta} \sum_{\omega_l} \sum_{\lambda_2 \lambda_3} e^{-i\omega_l \eta} v_{[\mu\lambda_2 \lambda_3 \nu]}^{(2)} \mathcal{G}[\Sigma^{\text{HFB}}]^{\lambda_2 \alpha_2}(\omega_l) \\ &\quad \times \delta\Sigma_{\alpha_2 \alpha_3} \mathcal{G}[\Sigma^{\text{HFB}}]^{\alpha_3 \lambda_3}(\omega_l) , \end{aligned} \quad (\text{D4})$$

which eventually simplifies to

$$\delta\mathcal{F}[\Sigma^{\text{HFB}}]_{\mu\nu} = \frac{1}{2} \sum_{\lambda_2 \lambda_3} v_{[\mu\nu \lambda_2 \lambda_3]}^{(2)} \Pi^{(\lambda_2, \alpha_2)(\lambda_3, \alpha_3)}(0) \delta\Sigma_{\alpha_2 \alpha_3} , \quad (\text{D5})$$

where we have used the antisymmetry property of the linear perturbation of the self-energy, as well as the energy representation of the bubble propagator, Π , in Eq. (112c). We rewrite the previous expression using multi-indices,

$$\delta\mathcal{F}[\Sigma^{\text{HFB}}]^M = \sum_N \left(\frac{1}{2} V^{(2)} \Pi(0) \right)^{MN} \delta\Sigma_N . \quad (\text{D6})$$

The Jacobian $J_{\mathcal{F}}[\Sigma^{\text{HFB}}]$ of \mathcal{F} at Σ^{HFB} thus reads

$$J_{\mathcal{F}}[\Sigma^{\text{HFB}}] = \frac{1}{2} V^{(2)} \Pi(0) . \quad (\text{D7})$$

Let us recall that a fixed point x_0 of a functional $g[x]$ is said to be stable if and only if

$$r(J_g[x_0]) < 1 . \quad (\text{D8})$$

In the case of \mathcal{F} , this means that the HFB self-energy is stable if and only if¹⁹

$$r \left(\frac{1}{2} \Pi(0) V^{(2)} \right) < 1 . \quad (\text{D10})$$

As a direct consequence, the stability of the HFB self-energy is equivalent to the convergence of the series of ladders at a Matsubara frequency of $\Omega_p = 0$. We have not been able to prove that the stability of the HFB self-energy is a sufficient condition for the ladders to converge at any Matsubara frequency Ω_p , unless further assumptions are made. Thus, to the best of our knowledge, the stability of the HFB self-energy is only a *necessary condition* for the series of ladders to converge at any energy.

2. Sufficient condition

In this section we demonstrate how the assumption of a stronger stability condition on the HFB self-energy allows us to prove the convergence of the ladders at *any* Matsubara frequency.

a. Rationale

Let us assume that, in addition of condition (D10), Σ^{HFB} is a fixed point of \mathcal{F} verifying the stronger stability constraint

$$\left\| \frac{1}{2} \Pi(0) V^{(2)} \right\|_{\mathcal{S}_\infty} < 1 . \quad (\text{D11})$$

We recall that $\|M\|_{\mathcal{S}_\infty}$ denotes the supremum of the singular values of an operator M , see Eq. (140). In practice, this means that we require the singular values of the Jacobian $J_{\mathcal{F}}[\Sigma^{\text{HFB}}]$ to be strictly smaller than 1. To prove that condition (D11) is sufficient for the series of ladders to converge, we prove in App. D2b the following lemma,

$$\forall \Omega_p, \left\| \frac{1}{2} \Pi(\Omega_p) V^{(2)} \right\|_{\mathcal{S}_\infty} \leq \left\| \frac{1}{2} \Pi(0) V^{(2)} \right\|_{\mathcal{S}_\infty} . \quad (\text{D12})$$

Then, using the useful property

$$\forall M, r(M) \leq \|M\|_{\mathcal{S}_\infty} , \quad (\text{D13})$$

we have

$$r \left(\frac{1}{2} \Pi(\Omega_p) V^{(2)} \right) \leq \left\| \frac{1}{2} \Pi(\Omega_p) V^{(2)} \right\|_{\mathcal{S}_\infty} \quad (\text{D14})$$

and the following implication is proven to hold

$$\left\| \frac{1}{2} \Pi(0) V^{(2)} \right\|_{\mathcal{S}_\infty} < 1 \implies \forall \Omega_p, r \left(\frac{1}{2} \Pi(\Omega_p) V^{(2)} \right) < 1 . \quad (\text{D15})$$

Therefore, the strong stability condition (D11) on the HFB self-energy is a *sufficient* condition for the series of ladders to converge at any energy.

b. Demonstration

To prove lemma (D12), we first decompose $\Pi(\Omega_p)$ in its eigenbasis. Let us recall that in the HFB approximation, the bubble propagator can be written as

$$\begin{aligned} \Pi_{MN}(\Omega_p) &= -\frac{1}{\beta} \sum_q (i\omega_q - (U + \Sigma^{\text{HFB}}))_{\mu_1 \nu_1}^{-1} \\ &\quad \times (i(\Omega_p - \omega_q) - (U + \Sigma^{\text{HFB}}))_{\mu_2 \nu_2}^{-1} , \end{aligned} \quad (\text{D16})$$

where the multi-indices are defined by

$$M \equiv (\mu_1, \mu_2) , \quad (\text{D17a})$$

$$N \equiv (\nu_1, \nu_2) . \quad (\text{D17b})$$

¹⁹ We recall that, for any operator A and B , we have

$$r(AB) = r(BA) . \quad (\text{D9})$$

For simplicity, we assume that the spectrum of $U + \Sigma^{\text{HFB}}$ is non-degenerate. Since $U + \Sigma^{\text{HFB}}$ is Hermitian, the decomposition of the analytic propagator in its eigenbasis reads

$$(z - (U + \Sigma^{\text{HFB}}))^{-1} = \sum_{\epsilon_i} \frac{P_i}{z - \epsilon_i}, \quad (\text{D18})$$

where ϵ_i are the real eigenvalues of $U + \Sigma^{\text{HFB}}$ and P_i are the Hermitian projectors on the associated eigenspaces. The Hermitian projectors verify

$$P_i P_j = \delta_{ij} P_i, \quad (\text{D19a})$$

$$P_i^\dagger = P_i. \quad (\text{D19b})$$

Plugging Eq. (D18) into Eq. (D16) and performing the Matsubara sum, we obtain the following expression for the bubble propagator:

$$\Pi_{MN}(\Omega_p) = \sum_{ij} (P_i)_{\mu_1 \nu_1} (P_j)_{\mu_2 \nu_2} \frac{1 - (f(\epsilon_i) + f(\epsilon_j))}{\epsilon_i + \epsilon_j - i\Omega_p}. \quad (\text{D20})$$

We can use this expression to rewrite the kernel of the T -matrix as

$$\begin{aligned} \frac{1}{2} (V^{(2)} \Pi(\Omega_p))_{MN} = \\ \frac{1}{2} \sum_{ij} \sum_{\lambda_1 \lambda_2} \left(v_{[\mu_1 \mu_2 \lambda_1 \lambda_2]}^{(2)} (P_i)^{\lambda_1}_{\nu_1} (P_j)^{\lambda_2}_{\nu_2} \right) \\ \times \frac{1 - (f(\epsilon_i) + f(\epsilon_j))}{\epsilon_i + \epsilon_j - i\Omega_p}. \end{aligned} \quad (\text{D21})$$

To study the singular values of the kernel $\frac{1}{2} \Pi(\Omega_p) V^{(2)}$, we must, by definition, study the spectrum of $\frac{1}{4} (\Pi(\Omega_p) V^{(2)})^\dagger (\Pi(\Omega_p) V^{(2)})$. Using the Hermitian property of $V^{(2)}$ and $\Pi(\Omega_p)$ we have

$$\frac{1}{4} (\Pi(\Omega_p) V^{(2)})^\dagger (\Pi(\Omega_p) V^{(2)}) = \frac{1}{4} V^{(2)} \Pi(-\Omega_p) \Pi(\Omega_p) V^{(2)}. \quad (\text{D22})$$

Then, from Eq. (D21), we have

$$\begin{aligned} \frac{1}{4} \left(V^{(2)} \Pi(-\Omega_p) \Pi(\Omega_p) V^{(2)} \right)_{MN} = \\ \frac{1}{4} \sum_{ij} \sum_{\lambda_1 \lambda_2} \sum_{\alpha_1 \alpha_2} \left(v_{[\mu_1 \mu_2 \lambda_1 \lambda_2]}^{(2)} (P_i)^{\lambda_1}_{\alpha_1} (P_j)^{\lambda_2}_{\alpha_2} \right) \\ \times (P_k)^{\alpha_1 \kappa_1} (P_l)^{\alpha_2 \kappa_2} v_{[\kappa_1 \kappa_2 \nu_1 \nu_2]}^{(2)} \\ \times \frac{1 - (f(\epsilon_i) + f(\epsilon_j))}{\epsilon_i + \epsilon_j + i\Omega_p} \frac{1 - (f(\epsilon_k) + f(\epsilon_l))}{\epsilon_k + \epsilon_l - i\Omega_p}. \end{aligned} \quad (\text{D23})$$

Using Eq. (D19a) the expression simplifies to

$$\begin{aligned} \frac{1}{4} \left(V^{(2)} \Pi(-\Omega_p) \Pi(\Omega_p) V^{(2)} \right)_{MN} = \\ \frac{1}{4} \sum_{ij} \sum_{\substack{\lambda_1 \lambda_2 \\ \kappa_1 \kappa_2}} \left(v_{[\mu_1 \mu_2 \lambda_1 \lambda_2]}^{(2)} (P_i)^{\lambda_1 \kappa_1} (P_j)^{\lambda_2 \kappa_2} v_{[\kappa_1 \kappa_2 \nu_1 \nu_2]}^{(2)} \right) \\ \times \frac{(1 - (f(\epsilon_i) + f(\epsilon_j)))^2}{(\epsilon_i + \epsilon_j)^2 + \Omega_p^2}. \end{aligned} \quad (\text{D24})$$

Using the idempotence of the projectors P_i we have

$$\begin{aligned} \frac{1}{4} \left(V^{(2)} \Pi(-\Omega_p) \Pi(\Omega_p) V^{(2)} \right)_{MN} = \\ \frac{1}{4} \sum_{ij} \sum_{\substack{\lambda_1 \lambda_2 \\ \kappa_1 \kappa_2}} \sum_{\alpha_1 \alpha_2} \left(v_{[\mu_1 \mu_2 \lambda_1 \lambda_2]}^{(2)} (P_i)^{\lambda_1}_{\alpha_1} (P_j)^{\lambda_2}_{\alpha_2} \right) \\ \times (P_i)^{\alpha_1 \kappa_1} (P_j)^{\alpha_2 \kappa_2} v_{[\kappa_1 \kappa_2 \nu_1 \nu_2]}^{(2)} \\ \times \frac{(1 - (f(\epsilon_i) + f(\epsilon_j)))^2}{(\epsilon_i + \epsilon_j)^2 + \Omega_p^2}. \end{aligned} \quad (\text{D25})$$

To make the structure of the previous expression clearer we introduce

$$(P_{ij}^{(2)})_{(\mu_1, \mu_2)(\nu_1, \nu_2)} \equiv (P_i)_{\mu_1 \nu_1} (P_j)_{\mu_2 \nu_2} \quad (\text{D26})$$

so that

$$\begin{aligned} \frac{1}{4} V^{(2)} \Pi(-\Omega_p) \Pi(\Omega_p) V^{(2)} = \frac{1}{4} \sum_{ij} V^{(2)} P_{ij}^{(2)} P_{ij}^{(2)} V^{(2)} \\ \times \frac{(1 - (f(\epsilon_i) + f(\epsilon_j)))^2}{(\epsilon_i + \epsilon_j)^2 + \Omega_p^2}. \end{aligned} \quad (\text{D27})$$

Since P_i is Hermitian (see Eq. (D19b)) so is $P_{ij}^{(2)}$, i.e.

$$P_{ij}^{(2)\dagger} = P_{ij}^{(2)}. \quad (\text{D28})$$

Therefore, using the fact that $V^{(2)}$ is Hermitian (see Eq. (113a)) we have

$$V^{(2)} P_{ij}^{(2)} P_{ij}^{(2)} V^{(2)} = \left(P_{ij}^{(2)} V^{(2)} \right)^\dagger \left(P_{ij}^{(2)} V^{(2)} \right) \quad (\text{D29})$$

which implies that $V^{(2)} P_{ij}^{(2)} P_{ij}^{(2)} V^{(2)}$ is Hermitian semi-definite positive, i.e.

$$V^{(2)} P_{ij}^{(2)} P_{ij}^{(2)} V^{(2)} \succeq 0. \quad (\text{D30})$$

Concretely, this means that

$$\left(V^{(2)} P_{ij}^{(2)} P_{ij}^{(2)} V^{(2)} \right)^\dagger = V^{(2)} P_{ij}^{(2)} P_{ij}^{(2)} V^{(2)} \quad (\text{D31})$$

and that for any $(2, 0)$ -tensor X we have, in any orthogonal basis,

$$\sum_{MN} (X^M)^* (V^{(2)} P_{ij}^{(2)} P_{ij}^{(2)} V^{(2)})^M_N X^N \geq 0. \quad (\text{D32})$$

To extract information on the eigenvalues from the Hermitian semi-definite positiveness property (D32), we study its consequence on the Rayleigh quotient. The Rayleigh quotient of a $(2, 2)$ -tensor t and a $(2, 0)$ -tensor X is defined in any orthogonal basis by

$$\mathcal{R}(t, x) \equiv \frac{\sum_{MN} (X^M)^* t^M_N X^N}{\sum_M (X^M)^* X^M}. \quad (\text{D33})$$

Using inequality (D32) and

$$0 \leq \frac{(1 - (f(\epsilon_i) + f(\epsilon_j)))^2}{(\epsilon_i + \epsilon_j)^2 + \Omega_p^2} \leq \frac{(1 - (f(\epsilon_i) + f(\epsilon_j)))^2}{(\epsilon_i + \epsilon_j)^2} \quad (\text{D34})$$

we find that, for any $(2, 0)$ -tensor X

$$\begin{aligned} \mathcal{R} \left(\frac{1}{4} V^{(2)} \Pi(-\Omega_p) \Pi(\Omega_p) V^{(2)}, X \right) \\ \leq \mathcal{R} \left(\frac{1}{4} V^{(2)} \Pi(0) \Pi(0) V^{(2)}, X \right). \end{aligned} \quad (\text{D35})$$

Since the supremum of the Rayleigh quotient is the spectral radius, i.e.

$$\begin{aligned} \sup_X \mathcal{R} \left(\frac{1}{4} V^{(2)} \Pi(-\Omega_p) \Pi(\Omega_p) V^{(2)}, X \right) \\ = r \left(\frac{1}{4} V^{(2)} \Pi(-\Omega_p) \Pi(\Omega_p) V^{(2)} \right), \end{aligned} \quad (\text{D36})$$

we obtain

$$\begin{aligned} r \left(\frac{1}{4} V^{(2)} \Pi(-\Omega_p) \Pi(\Omega_p) V^{(2)} \right) \\ \leq r \left(\frac{1}{4} V^{(2)} \Pi(0) \Pi(0) V^{(2)} \right). \end{aligned} \quad (\text{D37})$$

Hence, we finally have proven that

$$\left\| \frac{1}{2} \Pi(\Omega_p) V^{(2)} \right\|_{\mathcal{S}_\infty} \leq \left\| \frac{1}{2} \Pi(0) V^{(2)} \right\|_{\mathcal{S}_\infty}. \quad (\text{D38})$$

Note that, with a similar analysis, we can make the stronger statement that $\left\| \frac{1}{2} \Pi(\Omega_p) V^{(2)} \right\|_{\mathcal{S}_\infty}$ is an even function of Ω_p which decreases for $\Omega_p > 0$.

3. Separable interaction

In this final section, we study the particular case where the interaction $V^{(2)}$ is separable. By separable we mean that we assume the existence of two $(0, 2)$ -tensors v and v' such that

$$V_{MN}^{(2)} = v_M v'_N. \quad (\text{D39})$$

We start from the stability condition (D10) on the HFB self-energy, Σ^{HFB} . Since $V^{(2)}$ is separable, so is the product $\frac{1}{2} \Pi(\Omega_p) V^{(2)}$ and we thus have

$$r \left(\frac{1}{2} \Pi(\Omega_p) V^{(2)} \right) = \left\| \frac{1}{2} \Pi(\Omega_p) V^{(2)} \right\|_{\mathcal{S}_\infty}. \quad (\text{D40})$$

Then, combining (D10) and Eq. (D40) with $\Omega_p = 0$, we obtain

$$\left\| \frac{1}{2} \Pi(0) V^{(2)} \right\|_{\mathcal{S}_\infty} < 1. \quad (\text{D41})$$

Using lemma (D12), we have

$$\left\| \frac{1}{2} \Pi(\Omega_p) V^{(2)} \right\|_{\mathcal{S}_\infty} \leq \left\| \frac{1}{2} \Pi(0) V^{(2)} \right\|_{\mathcal{S}_\infty} < 1. \quad (\text{D42})$$

Eventually, using again Eq. (D40), we find that

$$r \left(\frac{1}{2} \Pi(\Omega_p) V^{(2)} \right) \leq r \left(\frac{1}{2} \Pi(0) V^{(2)} \right) < 1. \quad (\text{D43})$$

Therefore, whenever the interaction is separable, the stability of the HFB self-energy is a *necessary and sufficient* condition to the convergence of the series of ladders at any energy.

-
- [1] M. Drissi, A. Rios, and C. Barbieri, “Nambu-Covariant Many-Body Theory I: Perturbative Approximations,” (2021).
- [2] V. Soma, T. Duguet, and C. Barbieri, *Phys. Rev. C* **84**, 064317 (2011).
- [3] T. Duguet and A. Signoracci, *J. Phys. G* **44**, 015103 (2016).
- [4] P. Navrátil, S. Quaglioni, I. Stetcu, and B. R. Barrett, *J. Phys. G* **36**, 083101 (2009).
- [5] R. Roth, J. Langhammer, A. Calci, S. Binder, and P. Navrátil, *Phys. Rev. Lett.* **107**, 072501 (2011).
- [6] B. R. Barrett, P. Navrátil, and J. P. Vary, *Prog. Part. Nucl. Phys.* **69**, 131 (2013).
- [7] J. J. Griffin and J. A. Wheeler, *Phys. Rev.* **108**, 311 (1957).
- [8] B. Bally and M. Bender, *Phys. Rev. C* **103**, 024315 (2021).

- [9] S. D. Glazek and K. G. Wilson, *Phys. Rev. D* **48**, 5863 (1993).
- [10] F. Wegner, *Ann. Phys. (Berl.)* **506**, 77 (1994).
- [11] S. Bogner, R. Furnstahl, and A. Schwenk, *Prog. Part. Nucl. Phys.* **65**, 94 (2010).
- [12] K. Tsukiyama, S. K. Bogner, and A. Schwenk, *Phys. Rev. Lett.* **106**, 222502 (2011).
- [13] K. Tsukiyama, S. K. Bogner, and A. Schwenk, *Phys. Rev. C* **85**, 061304 (2012).
- [14] H. Hergert, S. K. Bogner, S. Binder, A. Calci, J. Langhammer, R. Roth, and A. Schwenk, *Phys. Rev. C* **87**, 034307 (2013).
- [15] S. K. Bogner, H. Hergert, J. D. Holt, A. Schwenk, S. Binder, A. Calci, J. Langhammer, and R. Roth, *Phys. Rev. Lett.* **113**, 142501 (2014).
- [16] I. Shavitt and R. J. Bartlett, *Many-Body Methods in Chemistry and Physics: MBPT and Coupled-Cluster Theory* (Cambridge University Press, 2009).
- [17] F. Coester, *Nucl. Phys.* **7**, 421 (1958).
- [18] F. Coester and H. Kümmel, *Nucl. Phys.* **17**, 477 (1960).
- [19] K. Kowalski, D. J. Dean, M. Hjorth-Jensen, T. Papenbrock, and P. Piecuch, *Phys. Rev. Lett.* **92**, 132501 (2004).
- [20] G. Hagen, T. Papenbrock, M. Hjorth-Jensen, and D. J. Dean, *Rep. Prog. Phys.* **77**, 096302 (2014).
- [21] J. M. Luttinger and J. C. Ward, *Phys. Rev.* **118**, 1417 (1960).
- [22] W. H. Dickhoff and H. Müther, *Rep. Prog. Phys.* **55**, 1947 (1992).
- [23] W. Dickhoff and C. Barbieri, *Prog. Part. Nucl. Phys.* **52**, 377 (2004).
- [24] C. Barbieri and A. Carbone, “Self-consistent green’s function approaches,” in *An Advanced Course in Computational Nuclear Physics: Bridging the Scales from Quarks to Neutron Stars*, edited by M. Hjorth-Jensen, M. P. Lombardo, and U. van Kolck (Springer International Publishing, Cham, 2017) pp. 571–644.
- [25] P. Demol, T. Duguet, A. Ekström, M. Frosini, K. Hebeler, S. König, D. Lee, A. Schwenk, V. Somà, and A. Tichai, *Phys. Rev. C* **101**, 041302 (2020).
- [26] A. Tichai, P. Arthuis, T. Duguet, H. Hergert, V. Somà, and R. Roth, *Phys. Lett. B* **786**, 195 (2018).
- [27] A. Signoracci, T. Duguet, G. Hagen, and G. R. Jansen, *Phys. Rev. C* **91**, 064320 (2015).
- [28] V. Somà, C. Barbieri, and T. Duguet, *Phys. Rev. C* **87**, 011303 (2013).
- [29] V. Somà, C. Barbieri, and T. Duguet, *Phys. Rev. C* **89**, 024323 (2014).
- [30] A. Tichai, P. Arthuis, H. Hergert, and T. Duguet, “ADG: Automated generation and evaluation of many-body diagrams III. Bogoliubov in-medium similarity renormalization group formalism,” (2021), [arXiv:2102.10889 \[nucl-th\]](https://arxiv.org/abs/2102.10889).
- [31] D. J. Dean and M. Hjorth-Jensen, *Rev. Mod. Phys.* **75**, 607 (2003).
- [32] M. Sigrist and K. Ueda, *Rev. Mod. Phys.* **63**, 239 (1991).
- [33] K. A. Brueckner, C. A. Levinson, and H. M. Mahmoud, *Phys. Rev.* **95**, 217 (1954).
- [34] K. A. Brueckner and C. A. Levinson, *Phys. Rev.* **97**, 1344 (1955).
- [35] H. A. Bethe, *Phys. Rev.* **103**, 1353 (1956).
- [36] B. D. Day and R. B. Wiringa, *Phys. Rev. C* **32**, 1057 (1985).
- [37] A. Rios, A. Polls, and W. H. Dickhoff, *Phys. Rev. C* **89**, 044303 (2014).
- [38] G. Baym, *Phys. Rev.* **127**, 1391 (1962).
- [39] P. Arthuis, T. Duguet, A. Tichai, R.-D. Lasserri, and J.-P. Ebran, *Comput. Phys. Commun.* **240**, 202 (2019).
- [40] A. Tichai, R. Wirth, J. Ripoché, and T. Duguet, *Eur. Phys. J. A* **56**, 272 (2020).
- [41] E. E. Salpeter and H. A. Bethe, *Phys. Rev.* **84**, 1232 (1951).
- [42] G. Baym and N. D. Mermin, *J. Math. Phys.* **2**, 232 (1961).
- [43] E. Economou, *Green’s Functions in Quantum Physics* (Springer, 2006).
- [44] G. Stefanucci and R. van Leeuwen, *Nonequilibrium Many-Body Theory of Quantum Systems: A Modern Introduction* (Cambridge University Press, 2013).
- [45] V. M. Galitskii and A. B. Migdal, *Sov. Phys. JETP* **7**, 18 (1958).
- [46] D. S. Koltun, *Phys. Rev. C* **9**, 484 (1974).
- [47] V. Somà and P. Božek, *Phys. Rev. C* **74**, 045809 (2006).
- [48] A. Rios, A. Polls, A. Ramos, and H. Müther, *Phys. Rev. C* **74**, 054317 (2006).
- [49] A. Rios, *Thermodynamical properties of nuclear matter from a self-consistent Green’s function approach*, Ph.D. thesis, University of Barcelona (2007).
- [50] A. Carbone, A. Cipollone, C. Barbieri, A. Rios, and A. Polls, *Phys. Rev. C* **88**, 054326 (2013).
- [51] J.-P. Blaizot and G. Ripka, *Quantum theory of finite systems* (MIT Press, Cambridge, Massachusetts, 1986).
- [52] I. S. Kac and M. G. Krein, *Amer. Math. Soc. Transl.*(2) **103**, 18 (1974).
- [53] A. Polls, A. Ramos, J. Ventura, S. Amari, and W. H. Dickhoff, *Phys. Rev. C* **49**, 3050 (1994).
- [54] P. Božek, *Phys. Rev. C* **65**, 054306 (2002).
- [55] J. B. French, *Course XXXVI: Many-body Description of Nuclear Structure and Reactions, Varenna 1965*, edited by C. Bloch, Proceedings of the International School of Physics Enrico Fermi (Academic Press, New York, 1966).
- [56] M. Baranger, *Nucl. Phys. A* **149**, 225 (1970).
- [57] T. Duguet and G. Hagen, *Phys. Rev. C* **85**, 034330 (2012).
- [58] T. Duguet, H. Hergert, J. D. Holt, and V. Somà, *Phys. Rev. C* **92**, 034313 (2015).
- [59] A. Rios, A. Carbone, and A. Polls, *Phys. Rev. C* **96**, 014003 (2017).
- [60] A. Rios, A. Polls, and H. Müther, *Phys. Rev. C* **73**, 024305 (2006).
- [61] F. Raimondi and C. Barbieri, *Phys. Rev. C* **99**, 054327 (2019).
- [62] J. Schirmer and G. Angonoa, *J. Chem. Phys.* **91**, 1754 (1989).
- [63] A. Ramos, A. Polls, and W. Dickhoff, *Nucl. Phys. A* **503**, 1 (1989).
- [64] P. Božek, *Phys. Rev. C* **59**, 2619 (1999).
- [65] A. Rios and V. Somà, *Phys. Rev. Lett.* **108**, 012501 (2012).
- [66] U. Fano, *Phys. Rev.* **124**, 1866 (1961).
- [67] G. Baym and L. P. Kadanoff, *Phys. Rev.* **124**, 287 (1961).
- [68] A. Cipollone, C. Barbieri, and P. Navrátil, *Phys. Rev. C* **92**, 014306 (2015).
- [69] C. De Dominicis and P. C. Martin, *J. Math. Phys.* **5**, 14 (1964).

- [70] C. De Dominicis and P. C. Martin, *J. Math. Phys.* **5**, 31 (1964).
- [71] P. C. Martin and J. Schwinger, *Phys. Rev.* **115**, 1342 (1959).
- [72] L. P. Kadanoff and P. C. Martin, *Phys. Rev.* **124**, 670 (1961).
- [73] E. Bergli and M. Hjorth-Jensen, *Ann. Phys. (N. Y.)* **326**, 1125 (2011).
- [74] C. Barbieri and W. H. Dickhoff, *Phys. Rev. C* **68**, 014311 (2003).
- [75] G. E. Brown and M. Bolsterli, *Phys. Rev. Lett.* **3**, 472 (1959).
- [76] M. Baranger, *Phys. Rev.* **120**, 957 (1960).
- [77] P. Nozières, *Theory of interacting Fermi systems* (Addison-Wesley, 1964).
- [78] R. Haussmann, *Z. Phys. B* **91**, 291 (1993).
- [79] R. Haussmann, *Self-consistent quantum-field theory and bosonization for strongly correlated electron systems* (Springer, Berlin, Heidelberg, 1999).
- [80] L. P. Kadanoff and G. Baym, *Quantum Statistical Mechanics* (Benjamin, New York, 1962).
- [81] W. D. Kraeft, D. Kremp, W. Ebeling, and G. Röpke, *Quantum Statistics of Charged Particle Systems* (Akademie-Verlag, Berlin, 1986).
- [82] D. J. Thouless, *Ann. Phys. (N. Y.)* **10**, 553 (1960).
- [83] R. Balian and M. Mehta, *Nucl. Phys.* **31**, 587 (1962).
- [84] R. Balian and M. Mehta, *Nucl. Phys.* **40**, 524 (1963).
- [85] G. C. Strinati, “Pairing Fluctuations Approach to the BCS–BEC Crossover,” in *The BCS–BEC Crossover and the Unitary Fermi Gas*, edited by W. Zwerger (Springer Berlin Heidelberg, Berlin, Heidelberg, 2012) pp. 99–126.
- [86] A. Perali, P. Pieri, G. C. Strinati, and C. Castellani, *Phys. Rev. B* **66**, 024510 (2002).
- [87] Y. Yanase and K. Yamada, *J. Phys. Soc. Jpn.* **68**, 2999 (1999).
- [88] J. Maly, B. Jankó, and K. Levin, *Physica C* **321**, 113 (1999).
- [89] S. Tsuchiya, R. Watanabe, and Y. Ohashi, *Phys. Rev. A* **80**, 033613 (2009).
- [90] F. Palestini and G. C. Strinati, *Phys. Rev. B* **89**, 224508 (2014).
- [91] G. C. Strinati, P. Pieri, G. Röpke, P. Schuck, and M. Urban, *Phys. Rep.* **738**, 1 (2018).
- [92] Q. Chen, J. Stajic, S. Tan, and K. Levin, *Phys. Rep.* **412**, 1 (2005).
- [93] S. Jensen, C. N. Gilbreth, and Y. Alhassid, *Eur. Phys. J. Spec. Top.* **227**, 2241–2261 (2019).
- [94] M. Randeria and E. Taylor, *Annu. Rev. Condens. Matter Phys.* **5**, 209 (2014).
- [95] D. Durel and M. Urban, *Universe* **6** (2020).
- [96] A. Schnell, G. Röpke, and P. Schuck, *Phys. Rev. Lett.* **83**, 1926 (1999).
- [97] M. Gaudin, *Nucl. Phys.* **20**, 513 (1960).
- [98] J. Schirmer, *Phys. Rev. A* **26**, 2395 (1982).
- [99] D. Danovich, *WIREs Comput. Mol. Sci.* **1**, 377 (2011).
- [100] M. Degroote, D. Van Neck, and C. Barbieri, *Phys. Rev. A* **83**, 042517 (2011).
- [101] C. Barbieri and W. H. Dickhoff, *Phys. Rev. C* **63**, 034313 (2001).
- [102] V. Somà, *Front. Phys. (Lausanne)* **8**, 340 (2020).
- [103] P. Arthuis, C. Barbieri, M. Vorabbi, and P. Finelli, *Phys. Rev. Lett.* **125**, 182501 (2020).
- [104] T. Frick and H. Mütter, *Phys. Rev. C* **68**, 034310 (2003).
- [105] A. Rios, A. Polls, A. Ramos, and H. Mütter, *Phys. Rev. C* **78**, 044314 (2008).
- [106] V. Somà and P. Božek, *Phys. Rev. C* **78**, 054003 (2008).
- [107] B. D. Day, *Rev. Mod. Phys.* **39**, 719 (1967).
- [108] T. Duguet, *J. Phys. G* **42**, 025107 (2014).
- [109] Y. Qiu, T. M. Henderson, J. Zhao, and G. E. Scuseria, *J. Chem. Phys.* **147**, 064111 (2017).
- [110] Y. Qiu, T. M. Henderson, T. Duguet, and G. E. Scuseria, *Phys. Rev. C* **99**, 044301 (2019).
- [111] N. Dunford and J. T. Schwartz, *Linear Operators. Part I: General Theory* (Interscience, New York, 1958).
- [112] A. E. Miroschnichenko, S. Flach, and Y. S. Kivshar, *Rev. Mod. Phys.* **82**, 2257 (2010).
- [113] A. R. P. Rau, *Phys. Scr.* **69**, C10 (2004).
- [114] C. Ott, A. Kaldun, P. Raith, K. Meyer, M. Laux, J. Evers, C. H. Keitel, C. H. Greene, and T. Pfeifer, *Science* **340**, 716 (2013).
- [115] B. Farid, “Ground and low-lying excited states of interacting electron systems: A survey and some critical analyses,” in *Electron Correlation in the Solid State* (Imperial College Press, 1999) Chap. 3, pp. 103–261.
- [116] A. I. Markushevich, *Theory of functions of a complex variable*, Selected Russian publications in the mathematical sciences, Vol. 2 (Prentice-Hall, Englewood Cliffs, NJ, 1965).
- [117] T. Kato, *Perturbation theory for linear operators* (Springer, Berlin, 1980).